Available online at www.sciencedirect.com

ScienceDirect

J. Differential Equations 258 (2015) 588–620

Journal of Differential Equations

www.elsevier.com/locate/jde

Cyclicity of a fake saddle inside the quadratic vector fields

P. De Maesschalck [a], S. Rebollo-Perdomo [b], J. Torregrosa [c,*]

[a] *Hasselt University, Martelarenlaan 42, B-3500 Hasselt, Belgium*
[b] *Centre de Recerca Matemàtica, 08193 Bellaterra, Barcelona, Spain*
[c] *Departament de Matemàtiques, Universitat Autònoma de Barcelona, Edifici C, 08193 Bellaterra, Barcelona, Spain*

Received 20 May 2014; revised 21 September 2014

Available online 16 October 2014

Abstract

This paper concerns the study of small-amplitude limit cycles that appear in the phase portrait near an unfolded fake saddle singularity. This degenerate singularity is also known as an impassable grain. The canonical form of the unperturbed vector field is like a degenerate flow box. Near the singularity, the phase portrait consists of parallel fibers, all but one of which have no singular points, and at the singular fiber, there is one node. We demonstrate different techniques in order to show that the cyclicity is bigger than or equal to two when the canonical form is quadratic.

MSC: 34C07; 37G10; 37G15; 34D15

Keywords: Cyclicity; Fake saddle; Impassable grain; Limit cycle; Bifurcation; Singularity unfolding

* Corresponding author.
E-mail addresses: peter.demaesschalck@uhasselt.be (P. De Maesschalck), srebollo@crm.cat (S. Rebollo-Perdomo), torre@mat.uab.cat (J. Torregrosa).

http://dx.doi.org/10.1016/j.jde.2014.09.024
0022-0396/

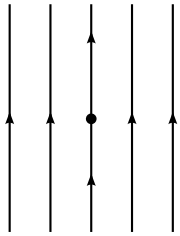

Fig. 1. Phase portrait of X_0.

1. Introduction

This paper concerns the study of small-amplitude limit cycles that appear in the phase portrait near an unfolded degenerate singularity. More specifically, we assume that the unperturbed vector field can be put in a form that is like a degenerate flow box: near the singularity, the phase portrait consists of parallel fibers, all but one of which have no singular points, and the singular fiber has a semi-stable equilibrium point. This singularity is known as a fake saddle or an impassable grain, see [24]. In fact, it is a singularity with exactly two saddle sectors.

Though the paper deals with more general vector fields, to present the ideas, consider the following typical model:

$$X_0: \{\dot{x} = 0,\ \dot{y} = x^2 + y^2\},$$

whose local phase portrait is shown in Fig. 1.

In any unfolding, the orbits $\{x = \text{const}\}$ away from the origin will smoothly be perturbed in a trivial way. Close to the origin, more complicated phenomena may occur: we show the presence of Hopf bifurcations, Bogdanov–Takens bifurcations, slow–fast (canard) behavior, homoclinic and heteroclinic orbits. All the above phenomena are well-known mechanisms near which limit cycles can be born, and in fact the study of periodic orbits near the degenerate point is the principle goal of this paper. We use the aforementioned mechanisms to show the presence of up to two small amplitude limit cycles, and provide evidence that by using these mechanisms this is the best cyclicity result one can get.

Determining an upper bound for the number of limit cycles turned out to be too difficult, as it was revealed that a multi-parameter global study of phase portraits was needed, going far beyond the traditional perturbative methods to create limit cycles.

In a study of unfoldings of a vector field like X_0, it is best to make a homogeneous (family) blow-up of the perturbed family of vector fields, thereby focusing on the behavior at the blow-up locus. The behavior at the blow-up locus has been shown to be mostly determined by perturbation terms of degree two and lower. *We will therefore focus our attention on perturbations of at most degree two.* Though this restriction immediately shows a relation between the Hilbert 16th problem in degree 2, the study of the singularity at X_0 has in fact no contribution in the degree-2 program outlined by Dumortier, Roussarie and Rousseau [14]. In that program, homogeneous vector fields could be avoided using rescalings. Setting this point aside, the study of the cyclicity of X_0 at the origin has a relevance by itself.

In Section 2 we consider forms for the unperturbed system under some additional generic and geometric constraints, and present a canonical form that depends on two parameters (A, B). Next, we present a reduction to canonical form of *the unfolding* of the degenerate singular point.

It is shown that a well-chosen canonical form of the unfolding is a 6-parameter family of vector fields: two parameters altering (A, B), and 4 additional parameters $(\mu_1, \mu_2, \mu_3, \mu_4)$. More precisely, we prove that any smooth unfolding can be brought into the following canonical form:

$$\begin{cases} \dot{x} = ax^2 + bxy + \mu_1 + \mu_2 x + \mu_3 y + O\big(\|(x, y)\|^3\big), \\ \dot{y} = x^2 + y^2 - \mu_4 + O\big(\|(x, y)\|^3\big), \end{cases} \tag{1}$$

where $a = A + o(1)$ and $b = B + o(1)$.

Normal forms for degenerate singularities have been studied before (see for example [1,26]). In this and in other papers, one typically cuts off the normal form, reducing it to the most dominant part (which is the quadratic part in this context). While in [26], one could actually realize this cut-off by proving the presence of a cutting-off coordinate transformation, proving that (1) is equivalent to its cut-off at degree 2 is not possible. See Remark 2 for a discussion.

The remainder of the paper deals with cyclicity results on the restriction of (1) to the class of quadratic vector fields. We present several results concerning the existence of limit cycles using perturbative arguments. In fact the maximum number of limit cycles obtained in this way is two, with configurations $(2 : 0)$ and $(1 : 1)$. In Section 3 we study the cyclicity and simultaneity properties near isolated singularities. We do this firstly by perturbing weak foci by computing Lyapunov coefficients, secondly by studying the presence of cusp points and their unfolding in a Bogdanov–Takens bifurcation diagram (in fact we prove the simultaneous existence of two BT-diagrams). A characterization of the centers of (1) restricted to the quadratic case can be found in Section 4. The quadratic perturbations of some centers included in these families have been studied by many authors. The Hamiltonian case is studied in [20] but the reversible non-Hamiltonian case has only been considered in few particular cases, see [4,6,17,21], and in all cases the cyclicity is two. A short review of these cases is also given in this section. In Section 5, we study slow–fast families of vector fields appearing in the model.

In a final step, inspired by [6], we consider in Section 6 a class of symmetric unfoldings of the singular point. The imposed symmetry allows us to reduce the dimension of the parameter space. As the unperturbed vector field is invariant under the transformation $(x, y, t) \mapsto (-x, -y, -t)$, we take the perturbations which are invariant under this transformation as well. Thus $\mu_2 = \mu_3 = 0$, and the restricted quadratic family (1) can be written as

$$\begin{cases} \dot{x} = ax^2 + bxy + \mu, \\ \dot{y} = x^2 + y^2 - 1. \end{cases} \tag{2}$$

We prove that this family has at most two limit cycles in configuration $(1 : 1)$. We show the limitations of the perturbative techniques as they fail to provide a global bifurcation diagram for the number of limit cycles even for this simple family of vector fields.

2. Reductions to canonical form

2.1. Canonical form of the unperturbed fake saddle

We consider a smooth vector field X_0 having a smooth invariant curve $x = \phi(y)$ (with $\phi(0) = 0$), and for which the reduction of X_0 to this curve is given by the equation

$$\dot{y} = cy^2 + O\big(y^3\big), \quad c > 0.$$

The conditions in the following lemma determine precisely the kind of singularity we examine in this paper.

Lemma 1. *Assume, under the above condition, that the origin is a degenerate singular point having exactly two separatrices, both of which are boundaries of two hyperbolic sectors. Then there exists a smooth local change of coordinates bringing the vector field into the form*

$$\begin{cases} \dot{x} = Ax^2 + Bxy + O\big(\|(x,y)\|^3\big), \\ \dot{y} = x^2 + y^2 + O\big(\|(x,y)\|^3\big), \end{cases} \tag{3}$$

where $A \geq 0$, $B < 1$ *and* $A^2 < 4(1-B)$. *(When the invariant fiber is a straight line, the change of coordinates is linear.)*

Proof. We assume that $X_0 = (P, Q)$ has a degenerate singular point at the origin, implying that $P(0,0) = Q(0,0) = 0$. We also assume that the degenerate point has no other separatrices beside the ones on the fiber $y = 0$, and that $\{y = 0\}$ separates two hyperbolic sectors. Since the origin is a degenerate singularity, a blow-up analysis reveals the nature of the singular point. We write

$$(x, y) = (r\cos\theta, r\sin\theta).$$

Imposing that $\{y = 0\}$ is the border of a hyperbolic sector has the implication $P_y(0,0) < 1$. (This is done by requiring the Jacobian matrix of the blow-up vector field at $(r, \theta) = (0, \pm\pi/2)$ to have a saddle structure.) Under this condition, we can apply a linear transformation $(x, y) \mapsto (x, \rho x + y)$ to make $Q_y(0,0) = 0$. Furthermore, we can then exclude the case $Q_x(0,0) = 0$ from the study (since there are always extra separatrices then), after which we can scale the coefficient to 1. In short, we can assume

$$P(x,y) = Ax^2 + Bxy, \qquad Q(x,y) = x^2 + y^2.$$

An additional search for separatrices would reveal the property $A^2 < 4(1-B)$. Symmetry allows us to assume $A \geq 0$. □

As a special case, we will sometimes consider those vector fields (3) that are invariant under the symmetry $(x, y, t) \mapsto (-x, -y, -t)$. The quadratic part is of course always invariant under the symmetry, but for some vector fields the higher order terms can break symmetry.

Remark 2. Lemma 1 shows that one can represent fake saddle singularities with a simple expression (3). We will not call this expression a normal form in this paper. Normal forms typically have a restricted definition and usually refer to Takens normal forms, Poincaré–Dulac normal forms, Birkhoff normal forms, or other specific normal forms. Though there are some works on normal forms of degenerate singular points [26,27], there is no convention on what could be called a normal form for a degenerate singularity. In this paper, we will often refer to (3) as a *canonical form*.

2.2. The degenerate flow-box property

The vector field (3) has the so-called *degenerate flow-box property*: there are two boxes $B_i \subset B_e$ (interior and exterior) with the following properties. Each of the boxes is diffeomorphic to a square, and its four boundaries consist of two orbits, an inset and an outset. Along the inset, the vector field is transverse and points inwards the box, and along the outside, the vector field is transverse and points outwards. The orbit-edges of B_i reach the outset of B_e in positive time and the inset of B_e in negative time. Furthermore, $B_e \setminus B_i$ has no singular points, and the size of the box B_i can be as small as desired.

Lemma 3. *Any smooth perturbation of vector field (3) retains the degenerate flow-box property.*

Proof. The boxes consist of regular orbits (which perturb to regular orbits), and insets and outsets. The transversality along the inset and outset also persists for small perturbations. □

Of course, the most interesting thing to study is what happens inside the interior box B_i for perturbations of (3). In the next section, we study unfoldings.

2.3. Canonical form for unfoldings of the fake saddle

We now consider a perturbation

$$\begin{cases} \dot{x} = Ax^2 + Bxy + \varepsilon P(x, y), \\ \dot{y} = x^2 + y^2 + \varepsilon Q(x, y). \end{cases}$$

We let

$$x = X + pY + q, \qquad y = Y + rX + s,$$

where p, q, r, s are to be determined implicitly below and keeping in mind all four ought to be $O(\varepsilon)$. For the new equations in (X, Y), we will require that

$$\frac{\partial \dot{Y}}{\partial X}(0,0) = \frac{\partial \dot{Y}}{\partial Y}(0,0) = \frac{\partial^2 \dot{Y}}{\partial X \partial Y}(0,0) = \frac{\partial^2 \dot{X}}{\partial Y^2}(0,0) = 0.$$

Considering the mapping $\Psi : (p, q, r, s, \varepsilon) \mapsto (\frac{\partial \dot{Y}}{\partial X}(0,0), \ldots, \frac{\partial^2 \dot{X}}{\partial Y^2}(0,0))$, then it is clear that $\Psi(0,0,0,0,0) = (0,0,0,0)$. On the other hand, it is a tedious but easy exercise to show that

$$\frac{\partial \Psi}{\partial (p, q, r, s)}(0) = \begin{vmatrix} 2(B-1) & 0 & 0 & 0 \\ 0 & 2 & 0 & 0 \\ 0 & 0 & 0 & 2 \\ 2 & 0 & 2-B & 0 \end{vmatrix} = 8(B-1)(B-2),$$

so we can apply the Implicit Function Theorem to prepare the perturbation in the required form. This implies that we may consider

$$\begin{cases} \dot{x} = ax^2 + bxy + \mu_1 + \mu_2 x + \mu_3 y + O\big(\|(x,y)\|^3\big), \\ \dot{y} = x^2 + y^2 - \mu_4 + O\big(\|(x,y)\|^3\big), \end{cases}$$

where $a = A + o(1)$, $b = B + o(1)$, and $a^2 < 4(1-b)$.

We now write

$$(\mu_1, \mu_2, \mu_3, \mu_4) = \big(v^2 M_1, v M_2, v M_3, v^2 M_4\big), \quad v \geq 0.$$

In a perturbation scheme where $\mu \approx 0$, we can keep $\|(M_1, M_2, M_3, M_4)\| = 1$ and let $v \approx 0$.

Lemma 4. *The ((v, M_1, M_2, M_3, M_4)-families of) boxes $B_i \subset B_o$ in (x, y)-space can be chosen so that B_i lies in an $O(v)$-neighborhood of the origin. (In the language of blow-up: in a family blow-up procedure, the interior box can be chosen as a compact $\mathcal{K}$ in the family chart.)*

Proof. Use phase directional blow-up and the fact that the equator only contains singularities at the poles. □

We now blow up the origin using a homogeneous family blow-up and consider the phase directional chart:

$$(x, y, v) = (vX, vY).$$

We find

$$\begin{cases} \dot{X} = aX^2 + bXY + M_1 + M_2 X + M_3 Y + O(v), \\ \dot{Y} = X^2 + Y^2 - M_4 + O(v). \end{cases} \tag{4}$$

Remark 5. It is clear that the behavior for $v = 0$ is the important piece of information needed to determine the behavior of (4). The system (4) with $v = 0$ has no singular points for $M_4 < 0$, and for $M_4 = 0$, it has a unique singular point at the origin, whose index is zero. Therefore, in both cases the restricted system has no limit cycles.

Remark 6. There is no hope of proving that (4) is in general equivalent to the truncated vector field with $v = 0$. In fact, this is only rarely true in versal unfoldings of degenerate singularities, and when one succeeds in proving so, it is due to restrictions on the complete family. This is shown for example in [26], where unfoldings of some degenerate singularities are discussed. In that paper, one considers unfoldings inside the class of vector fields that keep $X = 0$ and $Y = 0$ invariant. In the most generic setting of a degenerate singularity, the presence of a singularity is robust under perturbations respecting the structure. Hence, extra structure allows to prove a versal unfolding of finite codimension in [26]. This is not possible here.

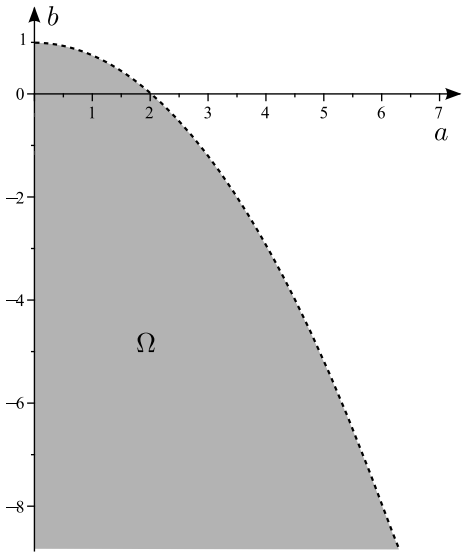

Fig. 2. Region of the parameters a and b.

2.4. Parameter charts of the quadratic canonical form

The canonical form obtained from (4), after reducing to $v = 0$, that can have limit cycles is

$$\begin{cases} \dot{X} = aX^2 + bXY + M_1 + M_2X + M_3Y, \\ \dot{Y} = X^2 + Y^2 - M_4, \end{cases} \tag{5}$$

with $M_4 \geq 0$.

Recall also that (M_1, M_2, M_3, M_4) lies on a sphere and cannot be zero simultaneously. It is important to realize that the local problem that was initially posed in this paper, i.e. study the cyclicity of the degenerate singular point, has now become a *global problem, both in phase space and parameter space.* The control on the number of limit cycles is typically not easy in this situation.

Removing the capitals in the notation, we have reduced the local cyclicity study to the global cyclicity study of the following family of vector fields:

$$\begin{cases} \dot{x} = ax^2 + bxy + \mu_1 + \mu_2x + \mu_3y, \\ \dot{y} = x^2 + y^2 - \mu_4, \end{cases} \tag{6}$$

where (x, y) is to be considered in a large compact set in the plane, and where the parameters $(\mu_1, \mu_2, \mu_3, \mu_4)$ lie on a sphere and cannot be zero simultaneously, and $(a, b) \in \Omega := \{(a, b) \in \mathbb{R}^2 \mid a \geq 0,\ a^2 + 4b - 4 < 0\}$, see Fig. 2.

In some cases, instead of working on a sphere, we prefer to work in one of the charts of the sphere: $\mu_4 = 1$ and $(\mu_1, \mu_2, \mu_3) \subset K \subset \mathbb{R}^3$, that is, we can consider the system

$$\begin{cases} \dot{x} = ax^2 + bxy + \mu_1 + \mu_2x + \mu_3y, \\ \dot{y} = x^2 + y^2 - 1, \end{cases} \tag{7}$$

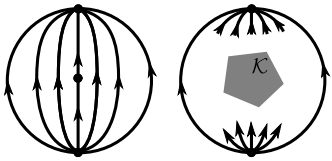

Fig. 3. Phase portrait of system (6) for the unperturbed one (left) and near the infinity (right).

where (x, y) lies in a large compact set in the plane, $(a, b) \in \Omega$, and $(\mu_1, \mu_2, \mu_3) \subset K \subset \mathbb{R}^3$ with K a large compact set as well. By choosing to work in this chart, we avoid the situation where $\mu_4 \approx 0$ and (μ_1, μ_2, μ_3) lies on a unit sphere. This choice is made for the sake of convenience and because it is to be expected that no additional phenomena are present there. With techniques similar to the ones proposed here, and by using extra desingularizations (blow-ups), a comprehensive study of the parameter chart $\mu_4 \approx 0$ is equally possible.

Following the techniques described in [12] the phase portraits near the infinity of the unperturbed and perturbed system (6) are drawn in Fig. 3. In particular the limit cycles will appear in a compact region $\mathcal{K}$ in the phase space, in correspondence with the findings in Lemma 4. Moreover, the total index of finite singularities is zero because the index of the fake saddle singularity of the unperturbed system (6) is also zero.

3. Limit cycles bifurcating from singularities

This section is devoted to the research on limit cycles that bifurcate from singularities. From previous section we know that the total index of all finite singularities is 0. This research is divided into two subsections. In the former we will study the maximum order of a weak focus (index $+1$). The latter deals with the study of Bogdanov–Takens bifurcation (index 0). In both cases we first study each point separately and then study simultaneous bifurcations.

3.1. Bifurcation from weak foci

Let X be the vector field associated with system (6). Then its linearization matrix at a point (x, y) is

$$DX(x, y) = \begin{pmatrix} 2ax + by + \mu_2 & bx + \mu_3 \\ 2x & 2y \end{pmatrix}.$$

Thus, the trace and the determinant of $DX(x, y)$ are denoted by

$$\operatorname{tr} DX(x, y) = 2(ax + by) + (2 - b)y + \mu_2, \tag{8}$$

$$\det DX(x, y) = 4y(ax + by) - 2b\left(x^2 + y^2\right) - 2\mu_3 x + 2\mu_2 y. \tag{9}$$

Lemma 7. *For a weak focus (x_0, y_0) of system (6) we have:*

(i) *The value x_0 is non-zero.*
(ii) *The first Lyapunov quantities are given by*

$$V_3 = -\frac{v_{30} - v_{31}a - v_{32}a^2}{8x_0\alpha_0^5}, \tag{10}$$

$$V_5 = -\frac{2x_0y_0v_{50} + v_{51}a + x_0y_0v_{52}a^2 - v_{53}a^3}{16x_0^3\alpha_0^7}, \tag{11}$$

where α_0 *is the positive square root of* $\det DX(x_0, y_0)$*, and*

$$\begin{aligned}
v_{30} &= 2x_0y_0(b+2)\big(4(1-b)x_0^2 + \alpha_0^2 + 4y_0^2\big),\\
v_{31} &= \big(\alpha_0^2 + 4y_0^2\big)^2 - 2b\big(12y_0^2 + \alpha_0^2\big)x_0^2,\\
v_{32} &= 4x_0y_0\big(\alpha_0^2 + 4y_0^2\big),\\
v_{50} &= \big(2x_0^2 + 4y_0^2 + \alpha_0^2\big)\big(4x_0^2 + 4y_0^2 + \alpha_0^2\big)(b+2),\\
v_{51} &= 8(b-2)(b-3)x_0^6 + \big(112(2-b)y_0^2 + 2\alpha_0^2\big(b^2 + 10 - 9b\big)\big)x_0^4\\
&\quad - 2\big(4y_0^2 + \alpha_0^2\big)\big(\alpha_0^2(1+b) - (13b+14)y_0^2\big)x_0^2 - \big(4y_0^2 + \alpha_0^2\big)^3,\\
v_{52} &= 48bx_0^4 - \big((32 - 152b)y_0^2 + 2\alpha_0^2(4-b)\big)x_0^2 - 13\big(4y_0^2 + \alpha_0^2\big)^2,\\
v_{53} &= 12x_0^2\big(x_0^2 + 3y_0^2\big)\big(4y_0^2 + \alpha_0^2\big).
\end{aligned}$$

Proof. When $x_0 = 0$ we have

$$\begin{aligned}
\operatorname{tr} DX(0, y_0) &= \mu_2 + by_0 + 2y_0 = 0,\\
\det DX(0, y_0) &= 2y_0(by_0 + \mu_2) = -4y_0^2 \le 0.
\end{aligned}$$

Consequently $(0, y_0)$ is not a weak focus (see [25]). This proves (*i*).

To prove statement (*ii*), we will first use a suitable linear transformation to bring system (6) in its Poincaré normal form.

By hypothesis $\operatorname{tr} DX(x_0, y_0) = 0$ and $\det DX(x_0, y_0) = \alpha_0^2$ for a value $\alpha_0 > 0$. Hence, from (8) and (9) it follows that

$$\mu_2 = -2(ax_0 + by_0) - y_0(2-b) \quad \text{and} \quad \mu_3 = -\frac{2bx_0^2 + \alpha_0^2 + 4y_0^2}{2x_0}.$$

On the other hand, since (x_0, y_0) is a singular point, from (6) we can easily see that

$$\mu_1 = \frac{2x_0^2(ax_0 + 2y_0) + 2bx_0^2 + \alpha_0^2 + 4y_0^2}{2x_0} \quad \text{and} \quad \mu_4 = \big(x_0^2 + y_0^2\big).$$

By using the linear transformation

$$u = \frac{x_0(x - x_0) + y_0(y - y_0)}{x_0}, \qquad v = \frac{\alpha_0(y - y_0)}{2x_0}$$

and the time reparametrization $d\tau = \alpha_0\, dt$, the system (6) becomes

$$\begin{cases} u' = -v + a_{20}u^2 + a_{11}uv + a_{02}v^2, \\ v' = u + b_{20}u^2 + b_{11}uv + b_{02}v^2, \end{cases} \tag{12}$$

where the prime denotes the derivative with respect to τ, and

$$a_{20} = \frac{ax_0 + y_0}{x_0\alpha_0}, \qquad a_{11} = \frac{2bx_0^2 - 4y_0(y_0 + ax_0)}{x_0\alpha_0^2},$$
$$b_{20} = \frac{1}{2x_0}, \qquad a_{02} = \frac{4y_0(y_0(y_0 + ax_0) + x_0^2(1-b))}{x_0\alpha_0^3},$$
$$b_{11} = \frac{2y_0}{x_0\alpha_0}, \qquad b_{02} = \frac{2(x_0^2 + y_0^2)}{x_0\alpha_0^2}.$$

The origin of this system corresponds to the point (x_0, y_0) of (6).

Finally, the expressions of the Lyapunov quantities V_3 and V_5 given in (10) and (11) follow after rewriting system (12) as

$$z' = iz + Az^2 + Bz\bar{z} + C\bar{z}^2$$

(with $z := u + iv$), applying [28, Proposition 1.2] and simplifying $V_5|_{V_3 \equiv 0}$. □

Theorem 8. *Let (x_0, y_0) be a weak focus of the perturbed system (6).*

(i) *if $a \neq 0$, then (x_0, y_0) is of order at most 2.*
(ii) *if $a = 0$, then (x_0, y_0) is of order at most 1 if $y_0 \neq 0$ and $b \neq -2$; otherwise (x_0, y_0) is a center.*

Proof. (*i*) It sufficient to show that if $V_3 = 0$, then $V_5 \neq 0$. This follows if the resultant of the numerators of V_3 and V_5 with respect to y_0 is a non-vanishing function. This resultant can be factored as

$$\operatorname{Res}(V_3, V_5, y_0) = a^{10}\alpha_0^{16}x_0^{20}(b-2)^2 R_1 R_2^2 R_3,$$

where

$$R_1 = 4\big(a^2 + b^2\big)x_0^2 + b^2\alpha_0^2, \qquad R_2 = 2a^2b + (b-1)(b+2)^2$$

and

$$R_3 = 5(3-b)\big(3(b+1)a^2 + 4(2b-1)^2\big)x_0^2 + \alpha_0^2\big(10b - 5 + 3a^2\big)^2.$$

By the assumption $a > 0$, and the fact that $x_0 \neq 0$ (Lemma 7), it is clear that $R_1 > 0$. To complete the proof we will prove that R_2 and R_3 do not vanish in Ω.

If $(a, b) \in \Omega$, then $a^2 < -4(b-1)$. Thus, $R_2 < (b-1)(b-2)^2 < 0$ in Ω because $b - 1 < 0$ and $b - 2 < -1$ in Ω.

Showing that $3(b+1)a^2+4(2b-1)^2$ and $3-b$ are positive in Ω, is sufficient to show that $R_3>0$ in Ω because $x_0\neq 0$. If $(a,b)\in\Omega$, then it is clear that $3-b>0$. Moreover, if $b\geq -1$, then $b+1\geq 0$, which implies that $3(b+1)a^2+4(2b-1)^2>0$; and if $b<-1$, then $-4ba^2<-16b(b-1)$, whereby

$$3(b+1)a^2+4(2b-1)^2=3(b+1)a^2-16b(1-b)+4>3a^2-ba^2>0.$$

(*ii*) We consider the equivalent system (12). For $a=0$, the Lyapunov quantity V_3 simplifies to

$$V_3=\frac{y_0(2+b)(4(1-b)x_0^2+\alpha_0^2+4y_0^2)}{4\alpha_0^5}.$$

Since in Ω we have $1-b>0$, the polynomial $4(1-b)x_0^2+\alpha_0^2+4y_0^2$ is positive because $\alpha_0>0$. Hence, as we are assuming that $y_0\neq 0$ and $b\neq -2$ we can conclude that $V_3\neq 0$. Therefore, the origin of (12) or equivalently the weak focus (x_0,y_0) of (6) is of the order 1 at most.

To complete the proof we will prove that if $y_0=0$ or $b=-2$, then (x_0,y_0) is a center. We will consider two cases.

Case 1. Suppose $y_0=0$. From the expression of (6) we find that $\mu_1+\mu_2x_0=0$ because $a=0$. On the other hand, from (8) we obtain $\operatorname{tr}DX(x_0,0)=\mu_2$, which is zero because $(x_0,0)$ is a weak focus. Thus, we obtain $\mu_1=\mu_2=0$. Hence the system (6) becomes

$$\begin{cases}\dot{x}=y(bx+\mu_3),\\ \dot{y}=x^2+y^2-\mu_4.\end{cases}\tag{13}$$

Thus, from (9) it follows that $\det DX(x_0,0)=-2(bx_0^2+\mu_3x_0)$ which must be positive because $(x_0,0)$ is a weak focus. Hence $b^2+\mu_3^2\neq 0$. We will prove that this system has a first integral.

When $b=0$ we can assume that $\mu_3\neq 0$ and e^{-2x/μ_3} is an integrating factor that provides

$$\frac{\mu_3(2\mu_4-2y^2-\mu_3^2-2x\mu_3-2x^2)}{4\,\mathrm{e}^{2x/\mu_3}}$$

as a first integral, which has either a minimum or a maximum at $(x_0,0)$. Therefore $(x_0,0)$ is a center singularity of the system.

If $b\neq 0$, then $(bx+\mu_3)^{-(b+2)/b}$ is an integrating factor and, consequently,

$$\frac{(b-2)(x^2+(y^2-\mu_4)(1-b))-\mu_3^2-2x\mu_3}{2(b-1)(b-2)(bx+\mu_3)^{\frac{2}{b}}}$$

is a first integral. Hence, if $(x_0,0)$ is a weak focus for the system, then the first integral has either a minimum or a maximum at $(x_0,0)$ which implies that $(x_0,0)$ is a center.

Case 2. Suppose $b=-2$. From (8) we get $\operatorname{tr}DX(x_0,y_0)=\mu_2$, which must be zero by the assumption on (x_0,y_0). Thus (6) becomes

$$\begin{cases}\dot{x}=-2xy+\mu_1+\mu_3y,\\ \dot{y}=x^2+y^2-\mu_4,\end{cases}\tag{14}$$

which is a Hamiltonian system with a Hamiltonian function

$$H(x, y) = \frac{x^3}{3} + xy^2 - \frac{\mu_3}{2}y^2 - \mu_4 x - \mu_1 y.$$

Therefore, if (x_0, y_0) is a weak focus of the system, it is a center singularity. □

Corollary 9. *If $a \neq 0$ then the perturbed system (6) has no centers bifurcating from the origin of the unperturbed system.*

Theorem 10. *If system (6) has two simultaneous weak foci, then each one of them has order 1 at most.*

Proof. If $a = 0$, then the assumption follows from statement (*ii*) of Theorem 8. Hence, for the rest of the proof we assume that $a \neq 0$.

Let (x_0, y_0) and (x_1, y_1) be two different weak foci of system (6). Using their characterization as singular points, together with (8) and (9), we find

$$\begin{aligned} ax_i^2 + bx_i y_i + \mu_2 x_i + \mu_3 y_i &= 0, \\ x_i^2 + y_i^2 - \mu_4 &= 0, \\ \mu_2 - \big(2ax_i + (b+2)y_i\big) &= 0, \\ \alpha_i^2 - 2x_i\mu_3 + 2bx_i^2 + 4y_i^2 &= 0, \end{aligned}$$

where $\alpha_i = \det DX(x_i, y_i) > 0$ for $i = 0, 1$. From these expressions we can write $\mu_1, \mu_2, \mu_3, \mu_4$, x_1, y_1, α_0, and α_1 as functions of (x_0, y_0, a, b). Of particular note we get

$$\begin{aligned} x_1 &= \frac{(4a^2 - (b+2)^2)x_0 + 4a(b+2)y_0}{4a^2 + (b+2)^2}, \\ y_1 &= \frac{4a(b+2)x_0 - (4a^2 - (b+2)^2)y_0}{4a^2 + (b+2)^2}. \end{aligned}$$

We denote by V_{j0} and V_{j1} the Lyapunov quantities of the weak focus (x_0, y_0) and (x_1, y_1), respectively. We note that the expression of V_{j1} for $j = 3, 5$ comes from (10) and (11) in Lemma 7 if we replace x_0, y_0, and α_0 by x_1, y_1, and α_1, respectively. Of particular note,

$$V_{30} = \frac{\widetilde{V} x_0((b+2)x_0 - 2ay_0)^2}{\alpha_0^5(4a^2 + (b+2)^2)^2}$$

and

$$V_{31} = \frac{\widetilde{V}((4a^2 - (b+2)^2)x_0 + 4a(b+2)y_0)((b+2)x_0 - 2ay_0)^2}{\alpha_1^5(4a^2 + (b+2)^2)^3}$$

where $\widetilde{V} = -a(b-2)(2ba^2 + 3b^2 + b^3 - 4)$.

We note that if $(b+2)x_0 - 2ay_0 = 0$, then that implies that $y_1 = y_0$ and $x_1 = x_0$, which contradicts our assumption $(x_0, y_0) \neq (x_1, y_1)$. Hence we have $(b+2)x_0 - 2ay_0 \neq 0$.

On the other hand, it is easy to see that the zero locus of $\widetilde{V}$ is outside of $\Omega \setminus \{a = 0\}$, and we know that $x_0 \neq 0$ and $x_1 \neq 0$, that is, $(4a^2 - (b+2)^2)x_0 + 4a(b+2)y_0 \neq 0$. Moreover, this implies that $V_{30} \neq 0$ and $V_{31} \neq 0$. Therefore, (x_0, y_0) and (x_1, y_1) are weak foci of order 1 at most. □

3.2. Bifurcation from nilpotent cusps

We consider cusp singularities in (7), i.e. singularities (x_0, y_0) where the determinant and the trace of the linearization are zero, but the linearization itself is not. It is an elementary computation to show that nilpotent singularities are located at $(x_0, y_0) = (\cos\theta, \sin\theta)$ when

$$\mu_1 = a\cos^2\theta + \left(2 + b\cos^2\theta\right)\tan\theta, \tag{15}$$

$$\mu_2 = -(b+2)\sin\theta - 2a\cos\theta, \tag{16}$$

$$\mu_3 = (2-b)\cos\theta - 2\cos^{-1}\theta. \tag{17}$$

Proposition 11. *Around a nilpotent singularity and for any $N \geq 2$, there exists a local set of coordinates bringing (7) locally in the form*

$$\begin{cases} \dot{x} = y, \\ \dot{y} = \displaystyle\sum_{k=2}^{N} \left(r_k x^k + s_k x^{k-1} y\right) + O\left(\left\|(x,y)\right\|^{N+1}\right), \end{cases} \tag{18}$$

where in particular

$$r_2 = 4\tan\theta\left(1 + a\sin\theta\cos\theta - b\cos^2\theta\right), \qquad s_2 = 2b\cos\theta - 4a\sin\theta + 4\cos\theta.$$

The two coefficients r_2 and s_2 only vanish simultaneously when both $b = -2$ and $\theta = 0 \pmod{\pi}$.

Proof. This proposition is even valid up to $N = \infty$ (this is a reduction to Liénard form, see for example [23]), and is well-known. Here we restrict ourselves to giving the procedure to normalize up to cubic terms, the general case being a direct generalization. We first write $(x, y) = (\tilde{y} + x_0, \tilde{x} + y_0)$ to put the singularity at the origin. Notice the exchange of the roles of x and y. After this, a linear change of coordinates $(\tilde{x}, \tilde{y}) = (2\cos\theta\bar{x}, -2\sin\theta\bar{x} + \bar{y})$ changes the linear part to $\left(\begin{smallmatrix} 0 & 1 \\ 0 & 0 \end{smallmatrix}\right)$. Finally, we write

$$\bar{x} = X + a_2 X^2, \qquad \bar{y} = Y + b_0 X^2 + b_1 XY + b_2 Y^2$$

and for suitable choices of (a_2, b_0, b_1, b_2) (easily found with the help of a symbolic math program) one can eliminate the quadratic terms in $\dot{X}$ and the term with y^2 in the $\dot{Y}$-equation. Let us finally mention that the system of equations $\{r_2 = 0, s_2 = 0\}$ is solved when either $\sin\theta = 0$ (in which case $b = -2$ follows) or $b = 2 + 2\cos^{-2}\theta > 2$, which is out of the parameter regime that we are considering. □

When both r_2 and s_2 are non-zero, the nilpotent singularity is of codimension 2, and upon varying the parameters it unfolds in a complete Bogdanov–Takens diagram. This is easy to see: the trace at the singular point is given by $2ax + (b+2)y + \mu_2$, and a similar expression is found for the determinant at the nilpotent point. Computing the Jacobian determinant of the mapping $(x_0, y_0, \mu_1, \mu_2) \mapsto (\dot{x}, \dot{y}, \mathrm{tr}, \det)|_{x=x_0, y=y_0}$, evaluated at a point $(x_0, y_0) = (\cos\theta, \sin\theta)$, and given the conditions (15), (16), and (17), gives $-4\tan\theta((b-2)\cos^2\theta - 2) \neq 0$ in the parameter domain under study and when $\theta \neq 0$. In other words when $\theta \neq 0$, the two parameters (μ_1, μ_2) can be used as versal parameters completely unfolding the nilpotent point. We conclude that (7) contains all the elements appearing in Bogdanov–Takens diagrams.

Remark 12. Similarly, the mapping $(x_0, y_0, \mu_1, \mu_2) \mapsto (\dot{x}, \dot{y}, \mathrm{tr}, \det)|_{x=x_0, y=y_0}$ is easily verified to be regular at nilpotent singularities, especially when $\mu_2 = \mu_3 = 0$, i.e. the case that appears in the reversible system (2). This shows that not only cusp singularities appearing in (2) unfold in full Bogdanov–Takens diagrams, but they do so even *inside* the family (2).

Moreover, we can show that simultaneous BT-bifurcations occur:

Proposition 13. *A nilpotent singularity* $(x_0, y_0) = (\cos\theta, \sin\theta)$ *occurs simultaneously with another nilpotent singularity at* $(x_1, y_1) = (\cos\phi, \sin\phi)$ *only when* $\theta = \phi + \pi \pmod{2\pi}$ *and*

$$a = \frac{(2\sin^2\theta - 1)\sin\theta}{\cos^3\theta}, \qquad b = -2\tan^2\theta, \qquad \mu_1 = \tan\theta, \qquad \mu_2 = \mu_3 = 0.$$

The quadratic normal forms of Proposition 11 at both points are then the same, and $r_2 = 4\sin\theta\cos^{-3}\theta$ *and* $s_2 = 4(1 - 2\sin^2\theta)\cos^{-3}\theta$. *In the parameter domain* $\{a \neq 0\}$, *simultaneously occurring nilpotent singularities are always of codimension* 2 *and they unfold completely and independently upon varying the four parameters* (a, b, μ_2, μ_3). *In particular this implies the presence of two small-amplitude limit cycles or saddle-homoclinics near the two cusp singular points.*

Proof. We express $(\dot{x}, \dot{y}, \mathrm{tr}, \det)$ at (x_0, y_0) and at (x_1, y_1) and get a system of eight polynomial equations, which we consider in eight variables y_0, x_1, y_1, a, b, μ_1, μ_2, μ_3, and treating for example $x_0 = \cos\theta$ as a parameter. A cumbersome computation shows that (x_0, y_0) necessarily equals $(\cos\theta, \sin\theta)$ and (x_1, y_1) equals $(\cos\phi, \sin\phi)$ with $\phi = \theta$ or $\phi = \theta + \pi$. From the same computation, we derive expressions for a and b, and using those expressions, we can simplify the known expressions for the quadratic coefficients r_2 and s_2. It is clear that $r_2 \cdot s_2 = 0$ only when $a = 0$. Finally, assume $\phi = \theta + \pi$ and both points are nilpotent. Computing $(\dot{x}, \dot{y}, \mathrm{tr}, \det)$ at both points $(x, y) = (\cos\theta, \sin\theta)$ and $(x, y) = (-\cos\theta, -\sin\theta)$ leads to a map from $(x_0, y_0, x_1, y_1, a, b, \mu_2, \mu_3)$ into $\mathbb{R}^8$. The Jacobian determinant of this map can be easily verified to be non-zero which implies that (a, b, μ_2, μ_3) independently control the two bifurcation parameters of the Bogdanov–Takens bifurcation plane for both points. □

Two simultaneously appearing nilpotent singular points of codimension bigger than 2 hence could occur only along $a = 0$. Let us finally state a result concerning the maximal codimension of any appearing nilpotent singularity in our system through the next two propositions:

Proposition 14. *A nilpotent singularity for which* $r_2 = 0$ *and* $s_2 \neq 0$ *is of codimension three at most, and around this point, (7) can be locally brought into the form*

$$\begin{cases} \dot{x} = y, \\ \dot{y} = s_2 xy + r_3 x^3 + \tilde{s}_3 x^2 y + O\big(\|(x,y)\|^5\big), \end{cases}$$

with s_2 as before and non-zero $r_3 = 4(b-2)$ and with $\tilde{s}_3 = s_3 - 3s_2 r_4/(5r_3)$. The singularity is of nilpotent saddle, focus or elliptic type (see [16]), depending on parameters $(s_2, \tilde{s}_3, r_3)$.

Proof. Starting from the Liénard form (18) of some degree $N \geq 5$, one can consider yet another transformation

$$x = X + c_2 X^2 + c_3 X^3.$$

A time change allows to keep $\dot{X} = y$. Tracking down the effect on the $\dot{y}$ equation, we can choose c_2 and c_3 to remove the terms of order 4. However, with this change, a term of order 3 changes from $s_3 x^2 y$ to $\tilde{s}_3 x^2 y$. The explicit expression for r_3 is obtained exactly as r_2 and s_2 are obtained in the proof of Proposition 11. (In fact, one finds that $r_3 = 8a \sin\theta \cos\theta + 4b(2\sin^2\theta - 1)$, which simplifies to $4(b-2)$ along $r_2 = 0$.) □

Proposition 15. *At a nilpotent singularity for which $s_2 = 0$ and $r_2 \neq 0$ (7) can be locally brought into the form*

$$\begin{cases} \dot{x} = y, \\ \dot{y} = r_2 x^2 + \tilde{s}_4 x^3 y + O\big(\|(x,y)\|^5\big), \end{cases} \tag{19}$$

with $\tilde{s}_4 = s_4 - s_3 r_3/r_2$. Except when $(a,b) = (0,-2)$, $\tilde{s}_4$ is never zero together with s_2 in the relevant parameter domain.

Proof. Just as in the previous proposition, we start with the Liénard form (18) of some degree $N \geq 5$, and we consider $x = X + c_2 X^2 + c_3 X^3$, this time combined with $y = Y + d_2 Y^2 + d_3 Y^3$. A time rescaling again allows us to keep $\dot{X} = Y$, and the coefficients c_2, c_3, d_2, d_3 are determined in order get $\dot{Y}$ in the required form. The exact expression for $\tilde{s}_4$ is quite long and we have chosen not to include it, as there are precise instructions on how to compute it. Algebraically, there are two disjoint curves where $\tilde{s}_4 = s_2 = 0$, and both of them lie outside the domain $\{b < 1, a^2 + 4(b-1) < 0\}$. □

We leave it to the interested reader to check whether or not a versal unfolding of the two codimension 3 situations described above is found in (7). Versal unfoldings of the situations described in Propositions 14 and 15 are found in [16] and [15], respectively. For $(a,b) = (0,-2)$, and for

$$(\mu_1, \mu_2, \mu_3) = \left(\frac{2\sin^3\theta}{\cos\theta}, 0, \frac{2\cos 2\theta}{\cos\theta}\right),$$

system (19) around the singular point $(x_0, y_0) = (\cos\theta, \sin\theta)$ degenerates further as $\tilde{s}_4 = 0$, and the study remains inconclusive. It is easy to conclude that topologically, the singularities are cusps, but the unfolding is less clear. However, from the previous section, we know that since also $\mu_2 = 0$, the system is Hamiltonian in that case.

4. Configuration of centers and their perturbations

This section deals with the centers of the family (7) and gives a review of known results concerning their quadratic perturbations.

Proposition 16. *System (7) can have a center only if it has the form*

$$\begin{cases} \dot{x} = y(bx + \mu_3), \\ \dot{y} = x^2 + y^2 - 1, \end{cases} \quad \text{with } b < 1 \text{ and } \mu_3 \in \mathbb{R}; \tag{20}$$

or

$$\begin{cases} \dot{x} = -2xy + \mu_1 + \mu_3 y, \\ \dot{y} = x^2 + y^2 - 1, \end{cases} \quad \text{with } \mu_1, \mu_3 \in \mathbb{R}. \tag{21}$$

The bifurcation diagrams of systems (20) and (21), as well as their different topological phase portraits on the Poincaré disc, are shown in Figs. 4 and 5, respectively. In particular,

(i) *system (20) has a center if and only if*

$$(\mu_3, b) \in \{b < 1\} \cap \big(\{\mu_3 - b > 0\} \cup \{\mu_3 + b < 0\}\big) \subset \mathbb{R}^2, \quad \text{and}$$

(ii) *system (21) has a center if and only if*

$$(\mu_1, \mu_3) \in \big\{\mu_1^2 < 1\big\} \cup \big(\{\mathcal{D} < 0\} \cap \{\mu_1 \geq 1\}\big) \subset \mathbb{R}^2,$$

where $\mathcal{D} = 64\mu_1^4 + \mu_1^2(\mu_3^4 - 80\mu_3^2 - 128) - (\mu_3 - 2)^3(\mu_3 + 2)^3$.

From this result we can classify the centers in three families: The non-reversible Hamiltonian ((21) with $\mu_1 \neq 0$), the reversible Hamiltonian ((20) with $b = -2$ or (21) with $\mu_1 = 0$), and the reversible non-Hamiltonian ((20) with $b \neq -2$). As we show in the proof below, if the Hamiltonian associated with (21) has four or two different real singular points, then it has four singular values (in the complex plane) for $\mu_1 \neq 0$. Then from [18] we see that at most two limit cycles can born from H_3 and H_5 under quadratic perturbations; in particular the cyclicity of the period annuli is at most 2. Moreover, in [22] it is proved that the cyclicity of the period annulus of H_4 is at most 2. The reversible Hamiltonian is studied in [5] proving that again the cyclicity of the period annuli of H_6 is two, when both are considered separately or simultaneously. However, the global cyclicity of H_4 and H_6 cannot be determined since limit cycles could bifurcate simultaneously from the cusp or from the heteroclinic connections, respectively. This problem remains open. The cyclicity of the period annuli in the reversible non-Hamiltonian case has only been considered in a few particular cases, and in all the cases again the cyclicity was two. See [4,6,17,21].

Proof of Proposition 16. From the proof of Theorem 8 we obtain that system (6) can have a center only if it writes as (13) or (14) which, after the rescaling introduced in Section 2.4, become (20) and (21), respectively. Moreover, by applying the map $(x, y, t) \to (-x, -y, -t)$

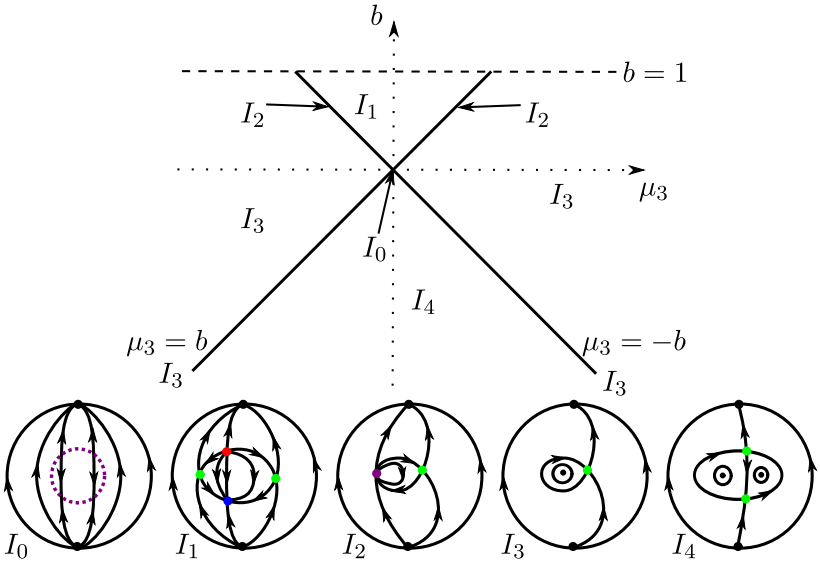

Fig. 4. Bifurcation diagram of system (20) and its different topological phase portraits.

we can assume, if necessary, $\mu_3 \geq 0$ in systems (20) and (21). Finally, as the singularities at infinity are hyperbolic, we restrict our analysis to the finite singularities that globally have a total index of zero, see Section 3.

We first study the bifurcation diagram and the phase portraits for system (20) considering the division of the parameter space according to the number and type of its singularities.

If $b = \mu_3 = 0$, then the circle $x^2 + y^2 = 1$ is a curve of singularities of the system, and every vertical straight line is invariant. Thus, the phase portrait is topologically conjugated to I_0 in Fig. 4.

For the remaining cases the points $(-1, 0)$ and $(1, 0)$, and the intersection points of $y = 0$ with the circle $x^2 + y^2 = 1$, are finite singularities of the system. Moreover, the system can have two additional singularities $(-\mu_3/b, y_i)$ for $i = 1, 2$ with $y_1 > 0$ and $y_2 < 0$, which are the intersection points of the invariant straight line $x = -\mu_3/b$ with the circle $x^2 + y^2 = 1$.

The next table shows the classification of the singularities of the system.

	$(-1, 0)$	$(1, 0)$	$(-\frac{\mu_3}{b}, y_1)$	$(-\frac{\mu_3}{b}, y_2)$
I_1	saddle	saddle	unstable node	stable node
I_2	$h - e$	saddle	–	–
I_3	center	saddle	–	–
I_4	center	center	saddle	saddle

where $h - e$ means one hyperbolic sector and one elliptic sector,

$$I_1 = \{(\mu_3, b) \mid b < 1,\ b > \mu_3\}, \qquad I_3 = \{(\mu_3, b) \mid b < 1,\ |b| < \mu_3,\ -b = \mu_3\},$$
$$I_2 = \{(\mu_3, b) \mid b < 1,\ b = \mu_3\}, \qquad I_4 = \{(\mu_3, b) \mid b < 1,\ \mu_3 < -b\}.$$

See Fig. 4.

The proof of the above classification follows from the Hartman–Grobmann Theorem for hyperbolic singularities and from Theorem 8 for centers. This completes the local study of the phase portraits in regions I_1, I_3 for $\mu_3 \neq -b$, and I_4. The same can be applied for $(1,0)$ in I_2 and $(-1,0)$ in I_3 when $\mu_3 = -b$. The remaining cases, i.e. $(1,0)$ in I_3 with $\mu_3 = -b$ and $(-1,0)$ in I_2, are nilpotent singularities. To determine the local behavior we must apply the results concerning the characterization of nilpotent singularities. See Section 3.4 and Theorem 3.5 in [12]. Alternatively, see [2, Ch. IX, Theorem 66].

The local phase portraits of the singularities determine the global ones for regions I_2 and I_3. The global phase portraits for regions I_1 and I_4 are determined by using the local phase portraits of the singularities and by keeping in mind the existence of an invariant straight line $x = -\mu_3/b$. See Fig. 4.

Secondly, we will study the bifurcation diagram and the phase portraits for system (21), which is a Hamiltonian system with a Hamiltonian function

$$H(x,y) = \frac{x^3}{3} + xy^2 - \frac{\mu_3}{2}y^2 - x - \mu_1 y. \tag{22}$$

As in the previous case, we first divide the parameter space into regions according to the number of singularities. This can be done by studying the intersection points of the two components of the vector field. That is a hyperbola or the product of two straight lines with the unit circle. Consequently, the number of finite singularities is $0, 1, 2, 3, 4$. Alternatively, such a division is given by the zero-locus of the discriminant of the resultant between the components of the vector field:

$$\begin{aligned}
&\Delta\big(\mathrm{Res}\big(-2xy + \mu_1 + \mu_3 y, x^2 + y^2 - 1, x\big), y\big) \\
&\quad = \Delta\big(4y^4 + \big(\mu_3^2 - 4\big)y^2 + 2\mu_1\mu_3 y + \mu_1^2, y\big) \\
&\quad = 256\mu_1^2\big(64\mu_1^4 + \mu_1^2\big(\mu_3^4 - 80\mu_3^2 - 128\big) - \big(\mu_3^2 - 4\big)^3\big) = 256\mu_1^2\mathcal{D}(\mu_1, \mu_3).
\end{aligned} \tag{23}$$

See Fig. 5.

We will describe the phase portraits and the bifurcation diagram in terms of the number of singularities. For simplicity, each region and the corresponding phase portrait are denoted by the same symbol.

In $H_0 = \{\mathcal{D} > 0, |\mu_1| > 1\}$ the conics do not intersect. Consequently, there are no finite singularities and the phase portrait is topologically equivalent to H_0 in Fig. 5.

The conics are tangent in only one point in $H_1 = \{\mathcal{D} = 0, |\mu_1| > 1\}$. The unique singularity is nilpotent and it is a cusp point because the vector field is Hamiltonian. The global phase portrait is topologically equivalent to H_1 in Fig. 5.

When there are at least two singularities we prove that the values of the Hamiltonian for two of them coincide only when $\mu_1 = 0$. Hence, only in this case, two singularities can be connected by an invariant curve. Writing the singularities as

$$(x_i, y_i) = \left(\frac{1 - t_i^2}{1 + t_i^2}, \frac{2t_i}{1 + t_i^2}\right), \quad i = 1, 2,$$

with $t_1 \neq t_2$, the values of μ_1 and μ_3 are uniquely determined in terms of t_1, t_2. Thus, the difference of the Hamiltonian at these points is

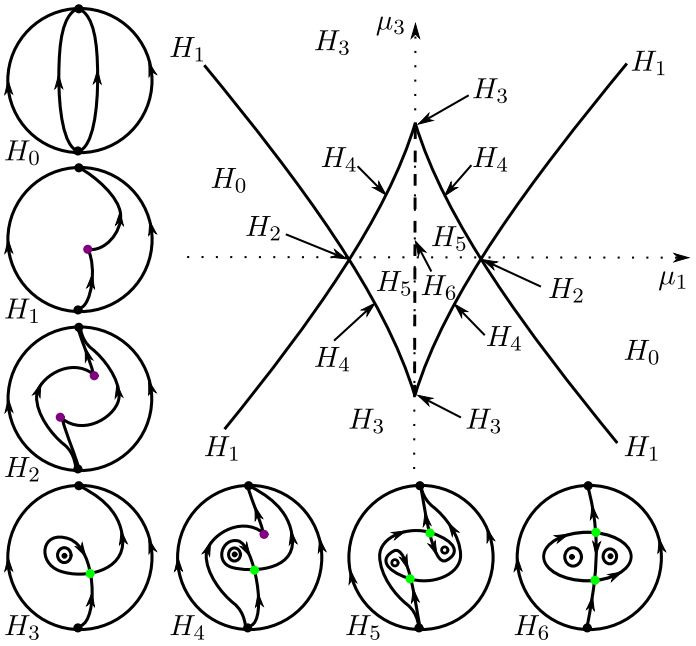

Fig. 5. Bifurcation diagram of system (21) and its different topological phase portraits. The curve $\mathcal{D} = 0$ is drawn as a continuous line.

$$\frac{4(t_1+t_2)(((3t_1^2+1)t_2-2t_1)^2+3(t_1^2+1)^2)(t_1-t_2)^3}{3(t_1^2+1)^3(t_2^2+1)^3(3t_1^2+1)},$$

which vanishes only when $t_1 = -t_2$, that is $x_1 = x_2$ and $y_1 = -y_2$, or equivalently $\mu_1 = 0$.

There are two different situations with two singular points. The first, in $H_2 = \{\mu_1 = \pm 1, \mu_3 = 0\}$, when the conics are tangent in two different points, and the second, in $H_3 = \{\mathcal{D} < 0\} \cup \{\mu_3 = \pm 2, \mu_1 = 0\}$, when the conics intersect transversally. In H_2 the singularities are of cuspidal type, using the same argument as in region H_1, and the global phase portrait is topologically equivalent to H_2 in Fig. 5 because the cusps are not connected. In H_3, the system is Hamiltonian. There, both singularities are simple, because the transversality, and of index $+1$ and -1 respectively. Consequently, they are of saddle and center type, and the global phase portrait is completely determined and it is topologically equivalent to H_3 in Fig. 5.

In $H_4 = \{\mathcal{D} = 0, 0 < |\mu_1| < 1\}$ the conics intersect in two transversal points and one tangent. The local behavior of these points is the same as the equivalent points in the previously studied cases. Then there are a cusp, a saddle and a center point. As the Hamiltonian at the cusp and the saddle do not coincide, the global phase portrait is topologically equivalent to H_4 in Fig. 5.

The remaining cases are the ones with four singularities. As the conics intersect transversally, the system is Hamiltonian and the total index is 0, we have two points with index $+1$ (centers) and two with index -1 (saddles). The global phase portrait depends on the value of the Hamiltonian at the saddle points. These values do not coincide in region $H_5 = \{\mathcal{D} > 0, 0 < |\mu_1| < 1\}$ and hence the saddles are disconnected. They coincide in region $H_6 = \{\mu_1 = 0, |\mu_3| < 2\}$. Additionally, in the last region, the system has a vertical invariant straight line that connect the saddles. The global phase portraits are topologically equivalent to H_5 and H_6 in Fig. 5, respectively. □

5. Singular perturbations

We consider

$$\begin{cases} \dot{x} = \varepsilon\big(ax^2 + bxy + \mu_1 + \mu_2 x + \mu_3 y\big), \\ \dot{y} = x^2 + y^2 - 1, \end{cases} \tag{24}$$

where ε is a small perturbation parameter. This system is obtained from (7) after rescaling the parameters by ε (and using the same symbols for the rescaled variants). Note that $(\varepsilon a, \varepsilon b) \in \Omega$ when $\varepsilon \geq 0$ is small enough.

This kind of system will be studied using techniques from geometric singular perturbation theory. This involves studying two limiting systems

$$\begin{cases} \dot{x} = 0, \\ \dot{y} = x^2 + y^2 - 1, \end{cases} \quad \text{and} \quad \begin{cases} \dot{x} = ax^2 + bxy + \mu_1 + \mu_2 x + \mu_3 y, \\ 0 = x^2 + y^2 - 1. \end{cases}$$

These two systems are called the fast reduced system and the slow reduced system. We define $C = \{(x, y): x^2 + y^2 = 1\}$ as the critical curve, a circle. Away from the singular points of the fast system, i.e. away from C, the dynamics of (24) is a perturbation of the dynamics of the fast system, whereas close to C, the dynamics of the slow system play a role. Of interest in C are two so-called contact points, located at $(x, y) = (\pm 1, 0)$. There, C is tangent to the vertical fibers of the fast subsystem, and the fast vector field has a nilpotent singular point (at other points of C, we have a partially hyperbolic singular point). The presence of contact points allows the possibility of the existence of slow–fast cycles of canard type. Before checking the conditions on the presence of canard cycles in detail, we prepare the computations by presenting expressions in polar coordinates. In polar coordinates $(x, y) = (r\cos\theta, r\sin\theta)$, we have

$$\begin{cases} \dot{r} = \big(r^2 - 1\big)\sin\theta + \varepsilon R(r, \theta)\cos\theta, \\ \dot{\theta} = \dfrac{r^2 - 1}{r}\cos\theta - \dfrac{\varepsilon}{r} R(r, \theta)\sin\theta, \end{cases}$$

with $R(r, \theta) = ar^2\cos^2\theta + br^2\cos\theta\sin\theta + \mu_1 + \mu_2 r\cos\theta + \mu_3 r\sin\theta$. Around partially hyperbolic points of C, the critical curve C perturbs to an ε-dependent invariant manifold. Using formal methods, it is easy to see that such invariant manifolds have the expression

$$r = 1 - \varepsilon\frac{\cos\theta}{2\sin\theta}\big(a\cos^2\theta + b\cos\theta\sin\theta + \mu_1 + \mu_2\cos\theta + \mu_3\sin\theta\big) + O\big(\varepsilon^2\big).$$

Note that the invariant manifolds potentially break down when $\sin\theta = 0$, e.g. at the contact points. For canard solutions to exist around the point $(x, y) = (+1, 0)$, it is clear that $a + \mu_1 + \mu_2 = o(1)$ as $\varepsilon \to 0$. We will prove in the next lemma that this is indeed a necessary condition. The fast subsystem is simply the reduction to $\varepsilon = 0$, while the slow subsystem can now be expressed in terms of θ:

$$\dot{\theta} = -\frac{a\cos^2\theta + b\cos\theta\sin\theta + \mu_1 + \mu_2\cos\theta + \mu_3\sin\theta}{\sin\theta}.$$

(We have plugged in the expression for the invariant manifold into the vector field to obtain this formula.) Checking near $\theta = 0$, this yields

$$\dot{\theta} = -\frac{a + \mu_1 + \mu_2}{\theta} - (b + \mu_3) + O(\theta). \tag{25}$$

We have already obtained heuristically that the first term should be zero. In that case it is clear that the second term should be positive: for a periodic orbit of slow–fast type to appear, the orbit has to go up along the circle slowly, and then go along a fast vertical fiber downwards to close the loop. These heuristical remarks can be made exact:

Lemma 17. *There exists a smooth function* $\lambda_+(\varepsilon, a, b, \mu_1, \mu_2, \mu_3)$ *that is* 0 *at* $\varepsilon = 0$ *and for which system* (24) *has canard cycles around* $(x, y) = (+1, 0)$ *when*

$$a + \mu_1 + \mu_2 = \lambda_+, \qquad b + \mu_3 < 0. \tag{26}$$

There exists a smooth function $\lambda_-(\varepsilon, a, b, \mu_1, \mu_2, \mu_3)$ *that is* 0 *at* $\varepsilon = 0$ *and for which system* (24) *has canard cycles around* $(x, y) = (-1, 0)$ *when*

$$a + \mu_1 - \mu_2 = \lambda_-, \qquad b - \mu_3 < 0. \tag{27}$$

Proof. We write $(x, y) = (1 + \tilde{y}, \tilde{x})$ and consider

$$\begin{cases} \dot{\tilde{x}} = 2\tilde{y} + \tilde{x}^2 + \tilde{y}^2, \\ \dot{\tilde{y}} = \varepsilon\big((a + \mu_1 + \mu_2) + (b + \mu_3)\tilde{x} + (\mu_2 + 2a + b\tilde{x})\tilde{y} + a\tilde{y}^2\big). \end{cases}$$

A well-known trick is to simply replace $a + \mu_1 + \mu_2$ by a new parameter which we call λ:

$$\begin{cases} \dot{\tilde{x}} = 2\tilde{y} + \tilde{x}^2 + \tilde{y}^2, \\ \dot{\tilde{y}} = \varepsilon\big(\lambda + (b + \mu_3)\tilde{x} + (\mu_2 + 2a + b\tilde{x})\tilde{y} + a\tilde{y}^2\big). \end{cases}$$

Properties of this new system, restricted to the parameter surface $\lambda = a + \mu_1 + \mu_2$, clearly imply similar properties of the original system. In this form we can readily apply Theorem 4 of [8]. It is easy to see that under the conditions of Lemma 17, all conditions of this theorem are verified. The theorem then implies the existence of canard cycles. This can also be done near $(x, y) = (-1, 0)$. □

Using the implicit function theorem, we can for example explicitly write μ_1 in terms of the other parameters so that (26) is satisfied, thereby showing the presence of canard cycles around $(x, y) = (+1, 0)$. Similarly for the left contact point. Also, considering (26) and (27) as a system of equations, the same implicit function theorem allows us to find an implicit solution by writing (μ_1, μ_2) in terms of the remaining parameters $(a, b, \mu_3, \varepsilon)$.

Lemma 17 shows the presence of a small-amplitude canard cycle near the contact point. The canard cycle consists of (a perturbation of) a fast vertical path connecting $(x, y) = (\cos\theta_0, \sin\theta_0)$ and $(x, y) = (\cos\theta_0, -\sin\theta_0)$, (for $\theta_0 \approx 0$ or $\theta_0 \approx \pi$) together with a small arc on the circle. The stability of the obtained periodic orbit can be computed using a slow divergence integral, see [7]. This integral is the divergence of the fast vector field, integrated along the slow arcs, and it is

well-known that it can be computed in arbitrary coordinate systems. In polar coordinates the divergence is given by $2y + O(\varepsilon) = 2\sin\theta + O(\varepsilon)$, so we define

$$I_+(\theta_0) = -\int_{-\theta_0}^{\theta_0} \frac{2\sin^2\theta}{a\cos^2\theta + b\cos\theta\sin\theta + \mu_1 + \mu_2\cos\theta + \mu_3\sin\theta}\,d\theta,$$

as the slow divergence integrals of slow–fast cycles around the contact point $(x, y) = (+1, 0)$, and

$$I_-(\theta_0) = -\int_{2\pi-\theta_0}^{\theta_0} \frac{2\sin^2\theta}{a\cos^2\theta + b\cos\theta\sin\theta + \mu_1 + \mu_2\cos\theta + \mu_3\sin\theta}\,d\theta,$$

for slow divergence integrals of slow–fast cycles around $(-1, 0)$. It is clear that these expressions only make sense when the integrand is well-defined for θ in the integration interval. We can now prove:

Proposition 18. *The coexistence of canard cycles around slow–fast Hopf points in a* $(1:1)$ *configuration in* (24) *occurs for any choice of* (a, b, μ_3) *with* $b < 0$ *and* $|\mu_3| < |b|$*, along a specific choice of* (μ_1, μ_2) *in terms of* $(\varepsilon, a, b, \mu_3)$ *and of the size of the cycles. In case of coexisting canard cycles, one always has a* $(1:1)$ *configuration when* $a \neq 0$*.*

Proof. From Lemma 17, we know that $b < 0$ and $|\mu_3| < -b$ must be satisfied for coexisting canard cycles to appear. Letting $\theta_+ \in (0, \pi)$ be an angle uniquely defining a canard cycle passing near the contact point $(x, y) = (+1, 0)$, and letting $\theta_- \in (0, \pi)$ be an angle uniquely defining a canard cycle passing near $(x, y) = (-1, 0)$, then Lemma 17 states that μ_1 and μ_2 are determined in terms of θ_+ and θ_- (and the other parameters), and that $(\mu_1, \mu_2) = (-a, 0) + o(1)$. The slow divergence is given by

$$I_+(\theta_+) = -\int_{-\theta_+}^{\theta_+} \frac{2\sin\theta}{\mu_3 + b\cos\theta - a\sin\theta}\,d\theta$$

(with a similar expression for $I_-(\theta_-)$). Observe that $\frac{\partial}{\partial a} I_+(\theta_+)$ is strictly positive and that $I_+(\theta_+) = 0$ at $a = 0$, which implies that the slow divergence integral has a fixed sign along θ_+. It follows, for $a \neq 0$, from results in [9] and [11] that the number of canard cycles around the contact point $(x, y) = (+1, 0)$ is one, i.e. we cannot have more than one canard cycle in each nest. The same is true for the contact point at $(x, y) = (-1, 0)$. □

In case $a = 0$ the coexisting canard cycles appear along $\mu_1 = \mu_2 = 0$; in that case we have a symmetric vector field, corresponding to the singularly perturbed center case. While the slow–fast center case has been studied before and some partial results could be obtained using the notion of slow divergence integral, the degenerate situation that appears in this context also needs to be studied when there are extra singularities in the slow dynamics (i.e. $\mu_3 + b\cos\theta_+ - a\sin\theta_+ = 0$). Though known results could be extended to such situations, there is no direct result

to fall back on. We have therefore decided to exclude the case $a = 0$ from the slow–fast study, though it should be clear that no phenomenon different from the case $a \neq 0$ is expected.

In the remainder we check the presence of a nest of $N \geq 2$ canard cycles around one of the contact points. In short we show that $N = 2$ appears and that it is the most logical upper bound to expect, though a full proof remains out of reach. Clearly, it is sufficient to deal with the cycles around $(x, y) = (+1, 0)$, so we assume that $a + \mu_1 + \mu_2 \approx 0$ and $b + \mu_3 < 0$. The slow divergence integral is expressed by

$$I(\theta_0) = \int_{-\theta_0}^{\theta_0} \frac{2\sin^2\theta}{a\sin^2\theta - b\cos\theta\sin\theta + \mu_2(1-\cos\theta) - \mu_3\sin\theta}\, d\theta.$$

Proposition 19. *Around a slow–fast Hopf point at $(x, y) = (+1, 0)$, there are at most two canard cycles.*

Proof. Clearly $I(0) = 0$, so any solution of $I = 0$ leads by Rolle to the existence of an intermediary solution of $I'(\theta_0) = 0$. Furthermore, if for any solution of $I' = 0$, we find $I''(\theta_0)$ has a fixed sign not depending on θ_0, then clearly there is only one such point and hence also at most only one solution of $I = 0$ (besides $\theta = 0$). By the results of [11], we know that this translates to the presence of at most two canard cycles. Let $N(\theta)$ be the denominator appearing in the integrand of I, i.e. $I(\theta) = \int_{-\theta_0}^{\theta_0} 2\sin^2\theta / N(\theta)\, d\theta$. We find

$$\begin{aligned} I'(\theta) &= \frac{2\sin^2\theta_0}{N(\theta_0)} + \frac{2\sin^2\theta_0}{N(-\theta_0)} = \frac{2\sin^2\theta_0}{N(\theta_0)N(-\theta_0)}\big(N(\theta_0) + N(-\theta_0)\big) \\ &= \frac{4\sin^2\theta_0}{N(\theta_0)N(-\theta_0)}(1-\cos\theta)(\mu_2 + a + a\cos\theta). \end{aligned}$$

A zero is found at $\theta = \theta_* := \arccos\frac{\mu_2+a}{-a}$, only when $-2a < \mu_2 < 0$ or $0 < \mu_2 < -2a$. A lengthy computation shows that

$$I''(\theta_*) = \sin\theta_* \frac{4a^2(\mu_2 + 2a)}{(b\mu_2 + ba - \mu_3 a)^2},$$

which has a fixed sign. This proves the proposition. □

Besides the canard cycles involved in this study, there can also be canard cycles at more degenerate contact points (not slow–fast Hopf): we distinguish in particular slow–fast Bogdanov–Takens points of codimension 2, and the more general slow–fast nilpotent contact points of codimension n.

Lemma 20. *At $(x, y) = (+1, 0)$, a slow–fast Bogdanov–Takens contact point appears when $(\mu_1, \mu_3) = (-a - \mu_2, -b) + o(1)$ and $\mu_2 \neq -2a$. A slow–fast contact point of codimension 3 appears when $(\mu_1, \mu_2, \mu_3) = (a, -2a, -b) + o(1)$ and $b \neq 0$. A slow–fast contact point of codimension 4 appears when $(\mu_1, \mu_2, \mu_3, b) = (a, -2a, 0, 0) + o(1)$. There are no slow–fast contact points of codimension higher than 4.*

Proof. Recall expression (25). Expanding it further in θ, a contact point of codimension n is found (for a definition, see [10]) when the first n coefficients of this expansion are zero. Hence, the lemma follows after an easy computation. □

The cyclicity near slow–fast contact points of codimension n is known up to $n = 3$. For $n = 1$, it is elaborated in [13], for $n = 2$ in [10], for $n = 3$ in the PhD thesis of R. Huzak (first part of the proof published in [19]). Using these results, it is possible to prove that the cyclicity near slow–fast contact points is at most 2. However, for slow–fast contact points of codimension 4, there are no results that can be applied.

6. The cyclicity of the reversible families

The quadratic family introduced in this paper has, basically, two symmetric subfamilies: (2) or (20). The objective of this section is to study the existence, nonexistence, uniqueness, and maximum number of limit cycles of the first subfamily with respect to the plane (a, b), because the cyclicity of the second one is zero since it has no limit cycles (see Proposition 16). First, we prove in Lemma 21, that (2) and (20) are the only reversible subfamilies. After that, we find the maximum number of limit cycles of (2), see Theorem 22. Then we restrict our analysis to $(a, b) \in \Omega$, where we prove that there are several regions in the parameter space (a, b, μ) such that (2) has no limit cycles, and finally, we prove that there is a region in the (a, b)-plane such that (2) has two limit cycles for suitable values of μ, always in the configuration $(1 : 1)$. These values correspond with Hopf and Bogdanov–Takens bifurcations.

Lemma 21. *Any system (6) which is invariant with respect to a point or a straight line can be transformed to (2) or (20), respectively.*

Proof. After a translation and a rotation of (6), the proof follows imposing the invariance of the transformed vector field with respect to $(x, y, t) \to (-x, -y, -t)$ or $(x, y, t) \to (x, -y, -t)$. □

Theorem 22. *System (2) has at most two limit cycles, and if it has limit cycles, then the only possible configuration is* $(1 : 1)$.

Proof. By using the change of variables $u = x$, $v = ax^2 + bxy + \mu$ system (2) becomes

$$\begin{cases} u' = buv, \\ v' = f(u, v)u^2 + g(u, v), \end{cases} \tag{28}$$

where

$$f(u, v) = \left(a^2 + b^2\right)u^2 + a(b - 2)v + 2\mu a - b^2$$

and

$$g(u, v) = (bv + v - \mu)(v - \mu).$$

Now, by applying the transformation $\{x = u^2, y = v\}$, the previous system reduces to

$$\begin{cases} x' = 2bxy, \\ y' = \big((a^2+b^2)x + a(b-2)y + 2\mu a - b^2\big)x + (by + y - \mu)(y - \mu), \end{cases}$$

which is a quadratic system with an invariant straight line. Therefore, the last system has at most one limit cycle. This implies that system (28) has at most 2 limit cycles, and if it has limit cycles the only possible configuration is $(1:1)$. This ends the proof of the first part of the statement because systems (28) and (2) are equivalent. □

As announced at the beginning of this section, we will study in detail system

$$\begin{cases} \dot{x} = ax^2 + bxy + \mu, \\ \dot{y} = x^2 + y^2 - 1, \end{cases} \tag{29}$$

when $(a, b) \in \Omega$. We note that some of the conclusions about nonexistence can also be extended to the full space (a, b, μ), but we are only interested in system (29) inside the class of system (6) as a perturbation of a fake saddle singularity, i.e. $(a, b) \in \Omega$.

The zero locus of

$$G(a, b) = 8a^2 + b^3 + 4b^2 + 4b \tag{30}$$

defines the points in the (a, b)-plane for which system (29) can exhibit cusp points, see the proof of Proposition 23. Hence, for analyzing the limit cycles of this system, we will split Ω into disjoint regions:

$$\begin{aligned} \mathcal{R}_0^0 &:= \big\{(a,b) \in \Omega \;\big|\; a = 0\big\}, \\ \mathcal{R}_0^+ &:= \big\{(a,b) \in \Omega \;\big|\; a \neq 0, 0 < b < 1, G(a,b) > 0\big\}, \\ \mathcal{R}_0^- &:= \big\{(a,b) \in \Omega \;\big|\; a \neq 0, b \leq 0, G(a,b) > 0\big\}, \\ \mathcal{R}_{11}^{\pm} &:= \big\{(a,b) \in \Omega \;\big|\; a \neq 0, \pm(2+b) > 0, G(a,b) < 0\big\}, \\ \Gamma^{\pm} &:= \big\{(a,b) \in \Omega \;\big|\; a \neq 0, \pm(2+b) > 0, G(a,b) = 0\big\}, \end{aligned} \tag{31}$$

see Fig. 6.

After the results and simulations of this section we can state that system (29) can only have limit cycles, always in configuration $(1:1)$, when the values of (a, b, μ) are in $\mathcal{R}_{11}^+$ and $\mu < 0$ or $\mathcal{R}_{11}^-$ and $\mu > 0$. In fact when $(a, b) \in \mathcal{R}_{11}^{\pm}$ the two limit cycles bifurcate simultaneously from two weak foci.

6.1. Local behavior of the singularities

This subsection deals with the number and local phase portrait of the singularities of system (29).

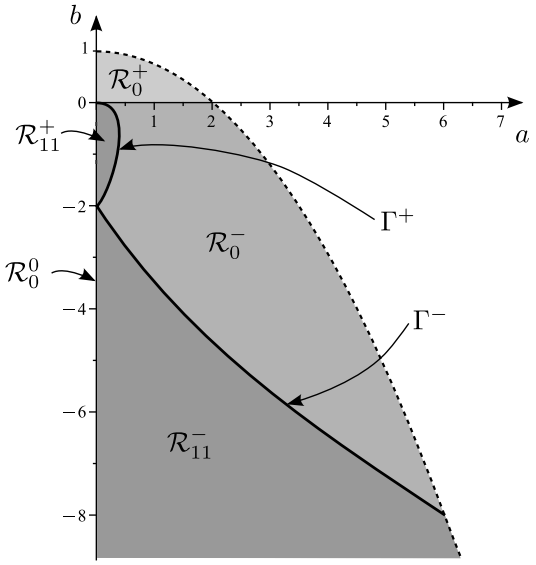

Fig. 6. Decomposition of Ω in the disjoint regions.

Proposition 23. *Consider $(a,b) \in \Omega$. When $(a,b) = (0,0)$, then system (29) has no finite singularities if $\mu \neq 0$ and otherwise the unit circle is filled with singularities. On the other hand, when $(a,b) \neq (0,0)$, consider $\mu^{\pm} = (-a \pm \sqrt{a^2+b^2})/2$, then the next properties hold.*

(i) *If $\mu \notin [\mu^-, \mu^+]$, then system (29) has no finite singularities.*
(ii) *If $\mu = \mu^{\pm}$, then system (29) has exactly two singularities. Moreover,*
- *when $(a,b) \in \Gamma^+$ and $\mu = \mu^-$, or $(a,b) \in \Gamma^-$ and $\mu = \mu^+$, both singularities are regular cusps;*
- *when $(a,b) = (0,-2)$, they are degenerate nilpotent singularities;*
- *in the remaining cases, they are saddle-nodes.*

(iii) *If $\mu \in (\mu^-, \mu^+)$, then system (29) has exactly four finite singularities: a pair of saddles and a pair of anti-saddles, located in the unit circle, and the points of each pair are antipodals.*

Proof. The statement for $(a,b) = (0,0)$ can be deduced directly from the structure of (29). From now on we assume that $(a,b) \neq (0,0)$.

The statement on the number of singularities follows directly studying the intersection points of the zero-locus of the components of the vector field: $ax^2 + bxy + \mu$ and the circle $x^2 + y^2 - 1$, and using the symmetry of system (29). A simple computation shows that the two zero-loci only intersect when $\mu \in [\mu^-, \mu^+]$. Moreover, when $\mu = \mu^{\pm}$ both curves are tangent in two antipodal symmetric points and when $\mu \in (\mu^-, \mu^+)$ there are two pairs of two antipodal points.

Since all the singularities lie on the unit circle, we can write each of them as

$$(x_0, y_0) = \left(\frac{1-t^2}{1+t^2}, \frac{2t}{1+t^2} \right),$$

with t a solution of $S = (a+\mu)t^4 - 2bt^3 + (-2a+2\mu)t^2 + 2bt + a + \mu = 0$. Then we have

$$\operatorname{tr} DX(x_0, y_0) = -2\frac{at^2 - (b+2)t - a}{t^2+1},$$
$$\det DX(x_0, y_0) = -2\frac{bt^4 + 4at^3 - 6bt^2 - 4at + b}{(t^2+1)^2}.$$

The resultant, with respect to the variable t, of the numerators of the above trace and determinant with S are $16T_{ab}^2$ and $4096(a^2+b^2)^2D_{ab}^2$, respectively, where $T_{ab} = (4a^2 + (b+2)^2)\mu - ab^2 + 4a$ and $D_{ab} = 4\mu^2 + 4a\mu - b^2$. Finally, the resultant, with respect to μ, of T_{ab} and D_{ab}, is $-G(a,b)^2$, see (30).

From the above resultants, we see that when $\mu \in (\mu^-, \mu^+)$, the determinant $\det DX(x_0, y_0)$ never vanishes. Consequently, the local behavior of all singularities is given by Hartman–Grobmann Theorem because of their hyperbolicity except in the weak focus case. But all the singularities are saddles or anti-saddles. The location on the circle follows from the work of Berlinskiĭ, see [3]. This concludes statements (i) and (iii).

When $\mu = \mu^{\pm}$, using the previous resultants, the determinant $\det DX(x_0, y_0)$ vanishes and the trace $\operatorname{tr} DX(x_0, y_0)$ only vanishes when $G(a,b) = 0$. Hence, when $G(a,b) \neq 0$ the points are semi-hyperbolic, in fact they are of saddle-node type, see [12].

The remaining cases are $\mu = \mu^{\pm}$ and $G(a,b) = 0$. We focus on $\mu = \mu^+$, the other case being completely the same. The set $\{G(a,b) = 0\} \cap \Omega = \Gamma^+ \cup \Gamma^- \cup \{(0,-2)\}$ is parameterized by $(a,b) = (\pm s(1-s^2), -2s^2)$, taking the $+$ sign and $s \in (0,1)$ for Γ^+, taking the $-$ sign and $s > 1$ along Γ^-, and $s = 1$ for $(a,b) = (0,-2)$. Solving $\{\dot{x} = 0, \dot{y} = 0, \operatorname{tr} DX = 0\}$ along Γ^+ with respect to (x, y, s) shows that solutions are only present when $\mu = -s$ (and along the solution also $\det DX = 0$). Evaluating the expression $\mu^+ = (-a + \sqrt{a^2+b^2})/2$ in this parameterized form along Γ^+ yields $\mu^+ = s^3 \neq -s = \mu$. On the other hand, solving $\{\dot{x} = 0, \dot{y} = 0, \operatorname{tr} DX = 0\}$ along Γ^- shows solutions along $\mu = s$, which corresponds to μ^+ when $s > 1$.

When $\mu = \mu^{\pm}$ and the trace is non-zero, the singularities are clearly semi-hyperbolic of saddle-node type. On the other hand, in the nilpotent case, one can apply Proposition 11, compute r_2 and s_2 along $\Gamma^{\pm}$ and one finds that $r_2 \cdot s_2$ is always non-zero, except when $(a,b,\mu) = (0,-2,\pm 1)$ (in that case, $s_2 = 0$ but $r_2 \neq 0$ since $\theta = \pm\pi/4$). Proposition 15 can be applied to see that it is a degenerate nilpotent singularity. □

6.2. *Nonexistence of limit cycles*

The next result describes the conditions on the parameter space where system (29) does not have limit cycles.

Theorem 24. *System (29) has no limit cycles in the cases:*

(i) $0 < b < 1$.
(ii) $a = 0$ *or* $b = 0$.
(iii) $\mu \notin (\mu^-, \mu^+)$.
(iv) $-2 \leq b < 0$ *and* $\mu \in [0, \mu^+)$, *or* $b \leq -2$ *and* $\mu \in (\mu^-, 0]$.
(v) $(a,b) \in \mathcal{R}_0^- \cap \{-2 \leq b < 0\}$ *and* $\mu \in (\mu^-, \hat{\mu}]$, *or* $(a,b) \in \mathcal{R}_0^- \cap \{b \leq -2\}$ *and* $\mu \in [\hat{\mu}, \mu^+)$, *where*

$$\hat{\mu} = \frac{a(b^2-4)}{4a^2 + (b+2)^2}.$$

Proof. (i) First, it is well-known that any limit cycle of a quadratic system has only one singularity of index one inside of it, and such a singularity is a focus. Hence, to prove this statement, it is enough to demonstrate that each singularity of (29), with $0 < b < 1$, is a saddle, or a node, or a saddle-node. We will split the proof of this case in two parts: $\mu = 0$ and $\mu \neq 0$.

Suppose now $\mu = 0$. Then, see Proposition 23, system (29) has four singularities, two of them on the line $\{x = 0\}$, which are $(0, 1)$ and $(0, -1)$, and the other two singularities are the intersections of the line $\{ax + by = 0\}$ and the circle $\{x^2 + y^2 = 1\}$, which we denote by p_1 and p_2. A straightforward computation of the trace and the determinant at these singularities, by using (8) and (9), and the Hartman–Grobmann Theorem implies that $(0, 1)$ and $(0, -1)$ are nodes, and that p_1 and p_2 are saddles.

Next suppose that $\mu \neq 0$. Let (x_0, y_0) be a singularity of (29). Since $\mu \neq 0$, $x_0 \neq 0$. Hence we have $y_0 = -(ax_0^2 + \mu)/bx_0$, and a simple computation shows that

$$\big(\mathrm{tr}^2\, DX - 4 \det DX\big)(x_0, y_0) = \frac{(a(b+2){x_0}^2 - \mu(b-2))^2 + 8b^3 x_0^4}{b^2 x_0^2}.$$

Thus, $(\mathrm{tr}^2\, DX - 4 \det DX)(x_0, y_0) > 0$ for $0 < b < 1$, which implies that (x_0, y_0) is a node if $\det DX(x_0, y_0) > 0$, and it is a saddle if $\det DX(x_0, y_0) < 0$. The case $\det DX(x_0, y_0) = 0$ follows from Proposition 23 and the point (x_0, y_0) is a saddle-node singularity. Thus, we have proved statement (i).

(ii) First, suppose $b = 0$. If $a = 0$, then (29) has no singularities; and if $a > 0$, then (29) has two invariant straight lines which contain all the singularities of the system. These properties imply that (29) has no limit cycles.

Suppose that $a = 0$. From previous cases we can assume $b < 0$. If $\mu = 0$, then the resulting system is a particular case of (20), which does not have limit cycles. If $\mu \neq 0$ and $f(x) = x^{-\frac{b+2}{b}}$, then we obtain

$$\mathrm{div}(fX) = -\frac{\mu(b+2)x^{-\frac{2(b+1)}{b}}}{b},$$

where $X = (P, Q)$ is the vector field associated with (29). Thus, $\mathrm{div}(fX)$ does not change sign for $x > 0$. Hence, the classical Bendixson–Dulac Theorem implies the assertion.

(iii) It follows from (i) and (ii) of Proposition 23 because in the first case system (29) has no singularities, and in the second one the type of singularities implies the nonexistence of limit cycles.

(iv) We can assume $b < 0$ and $a > 0$. By using the function $f(x) = x^{-\frac{b+2}{b}}$ we obtain

$$\mathrm{div}(fX) = -\frac{x^{-\frac{2(b+1)}{b}}}{b}\big(a(2-b)x^2 + \mu(b+2)\big).$$

Hence, if $-2 \leq b < 0$ and $\mu \geq 0$, then $\mathrm{div}(fX) \geq 0$ for $x > 0$; and if $b \leq -2$ and $\mu \leq 0$, then $\mathrm{div}(fX) \geq 0$ for $x > 0$. Thus, the Bendixson–Dulac Theorem implies that system (29) has no limit cycles.

(v) As $\mu \neq 0$ the y-axis is without contact with respect to the vector field. By symmetry we can restrict our analysis to the half plane $x > 0$. In this region, system (29) has one saddle and one anti-saddle, see Proposition 23. The straight line, L_{0S}, joining the origin and the saddle

point also passes through the other saddle. Consequently, as the vector field is quadratic, L_{0S} has no tangent points except the saddle point and the limit cycle cannot cross it. Hence the limit cycle remains, if it exists, in the angular region defined by L_{0S} and the y-axis that contains the anti-saddle point. The proof follows because, for the values of the parameters, the line where the trace vanishes does not intersect this angular region. □

6.3. Hopf and Bogdanov–Takens bifurcations

From Theorem 24 it follows that system (29) can only exhibit limit cycles when $\mu \in (\mu^-, \mu^+)$. Next, we prove the existence of a Bogdanov–Takens bifurcation curve and a Hopf bifurcation surface.

Theorem 25. *For each $(a_0, b_0) \neq (0, -2)$ in $\Gamma^+(\Gamma^-)$ there exists $\mu_0 < 0$ ($\mu_0 > 0$) such that system (29) undergoes two simultaneous Bogdanov–Takens bifurcations on $\mathcal{R}_{11}^+$ ($\mathcal{R}_{11}^-$).*

Theorem 26. *System (29) undergoes two simultaneous non-degenerate Hopf bifurcations on the surface*

$$\mu = \frac{a(b^2-4)}{4a^2+(b+2)^2} \tag{32}$$

if and only if $(a, b) \in \mathcal{R}_{11}^{\pm}$.

A direct consequence of the above two theorems is the next result.

Corollary 27. *For each (a, b) in $\mathcal{R}_{11}^+$ ($\mathcal{R}_{11}^-$), there are values of $\mu < 0$ ($\mu > 0$) such that system (29) has two limit cycles in configuration* (1 : 1).

Proof of Theorem 25. We focus on Γ^+, where we write

$$(a, b) = \left(s\left(1-s^2\right), -2s^2\right), \quad 0 < s < 1$$

(see the proof of Proposition 23), and find singularities of nilpotent type when $\mu = -s$ at $(x, y) = (\cos\theta, \sin\theta)$ when $\tan\theta = -s$. A lengthy computation of r_2 and s_2 from Proposition 11 shows that $r_2 s_2 \neq 0$ whenever $(a, b) \neq (0, -2)$ (i.e. whenever $s \neq 1$). Using Remark 12, we know that regular cusps appearing in the family (29) unfold completely according to a Bogdanov–Takens diagram inside the family (29). This proves the theorem. □

Proof of Theorem 26. Let $X = (P, Q)$ be the vector field associated with system (29). This system has critical points with a vanishing trace when $\{(x, y) \in \mathbb{R}^2 \mid P(x, y) = Q(x, y) = \operatorname{tr} DX(x, y) = 0\}$. A necessary condition so that the previous set is not empty is

$$\operatorname{Res}\left(\operatorname{Res}(P, \operatorname{tr} DX, y), \operatorname{Res}(Q, \operatorname{tr} DX, y), x\right) = 0.$$

The surface (32) follows from the above equation when $b \neq -2$. We choose μ^* such that (a, b, μ^*) is in this surface, then the change

$$(a,b)=\left(\frac{r(1-t^2)}{2(t^2+1)},\frac{2rt}{t^2+1}-2\right)$$

with $r>0$ and $-1<t<1$, means that the singularities of (29) can be written as

$$p_t^{\pm}=\pm\left(\frac{2t}{t^2+1},\frac{t^2-1}{t^2+1}\right),$$
$$q_t^{\pm}=\pm\left(\frac{2(-2t^2+rt-2)(t^2-1)}{(t^2+1)\sqrt{F}},\frac{rt^4-8t^3+6rt^2-8t+r}{(t^2+1)\sqrt{F}}\right),$$

with $F=r^2t^4+14r^2t^2-32rt^3+16t^4+r^2-32rt+32t^2+16$. Straightforward computations show that, when $a\neq 0$, $F>0$. Moreover, the function $G(a,b)$, defined in (30), moves to

$$G(r,t)=\frac{2r^2(t^6+4rt^3-5t^4-5t^2+1)}{(t^2+1)^3}.$$

The trace and the determinant at the singularities, see (8) and (9), are

$$\operatorname{tr}\left(p_t^+\right)=0,\qquad \det\left(p_t^+\right)=-\frac{2G(r,t)}{r^2},$$
$$\operatorname{tr}\left(q_t^+\right)=\pm\frac{2(t^2+1)^2G(r,t)}{r\sqrt{F(r,t)}},\qquad \det\left(q_t^+\right)=\frac{2G(r,t)}{r^2}.$$

Their sign is given in the next table:

	If $G(r,t)<0$		If $G(r,t)>0$	
	tr	det	tr	det
p_t^+	0	>0	0	<0
p_t^-	0	>0	0	<0
q_t^+	<0	<0	>0	>0
q_t^-	>0	<0	<0	>0

If $G(r,t)<0$ and $a\neq 0$ then Theorem 8(i) asserts that p_t^+ is not a center. Consequently, its stability is determined and $p_t^{\pm}$ are weak foci. If $G(r,t)>0$ there are no weak foci because $p_t^{\pm}$ are saddles. Thus, there are no Hopf bifurcations if $(a,b)\in\mathcal{R}_0^{\pm}$.

Finally, we show that two Hopf bifurcations exist when $G(r,t)<0$, that is, when $(a,b)\in\mathcal{R}_{11}^{\pm}$. Let ε be a small parameter. Thus, system (29) with $\mu=\mu^*+\varepsilon$ has a critical point, $(x_\varepsilon,y_\varepsilon)$, close to p_t^+, and a straightforward computation shows that

$$x_\varepsilon=\frac{2t}{t^2+1}+\varepsilon\frac{(t^2-1)(t^4+2t^2+1)}{2(t^6+4rt^3-5t^4-5t^2+1)}+O\left(\varepsilon^2\right),$$
$$y_\varepsilon=\frac{t^2-1}{t^2+1}-\varepsilon\frac{t(t^4+2t^2+1)}{t^6+4rt^3-5t^4-5t^2+1}+O\left(\varepsilon^2\right).$$

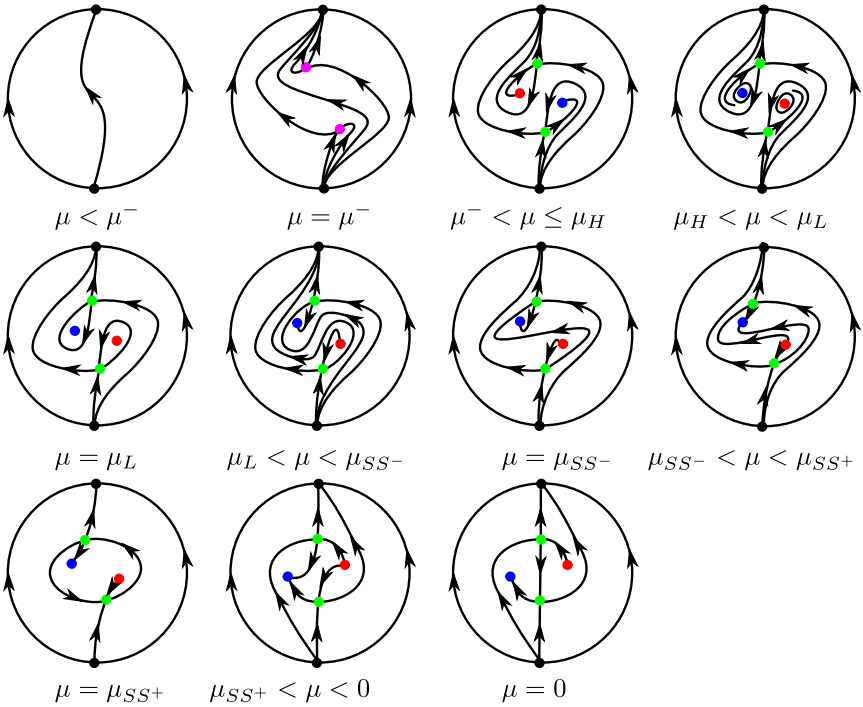

Fig. 7. Phase portraits evolution, for $\mu \leq 0$ when $(a, b) \in \mathcal{R}_{11}^+$.

This implies that $\mathrm{tr}(DX)(x_\varepsilon, y_\varepsilon) = -(r^3/G(r,t))\varepsilon + O(\varepsilon^2)$. Therefore, when we cross the surface (32), a critical point of focus type of system (29) changes the stability and, as it is not a center on the surface, a limit cycle bifurcates from p_t^+. At the same time, and with opposite stability, another one bifurcates from p_t^-. □

6.4. Phase portraits

From the previous sections, system (29) exhibits limit cycles when $(a, b) \in \mathcal{R}_{11}^+$ and $\mu < 0$ or when $(a, b) \in \mathcal{R}_{11}^-$ and $\mu > 0$. Figs. 7 and 8 shows phase portraits of the systems in these parameter regions. We have only shown these transitions because they are the only ones that, with our results and simulations, exhibit limit cycles. We think that there are no other bifurcations nor phase portraits in these parameter regions.

We explain these transitions following the results of the previous sections and some simulations using the software `P4`, see [12].

Assume that $(a, b) \in \mathcal{R}_{11}^+$. When $\mu < \mu^-$ there are no critical points, see Proposition 23. For $\mu < \mu^-$ two symmetric saddle-nodes appear that bifurcate into a pair: a symmetric saddle point and an anti-saddle point. For $\mu = \mu_H$, see Theorem 26, the system has two symmetric weak foci and two symmetric small limit cycles bifurcate from them, both of which remain present for $\mu_H < \mu < \mu_L$. The limit cycles grow in amplitude and disappear in two finite symmetric homoclinic connections for $\mu = \mu_L$. Then two types of finite saddle connections appear for $\mu = \mu_{SS^-}$ and $\mu = \mu_{SS^+}$. When $\mu = 0$, $x = 0$ is an invariant straight line (see Theorem 24), the points on this line are saddles and there are no limit cycles.

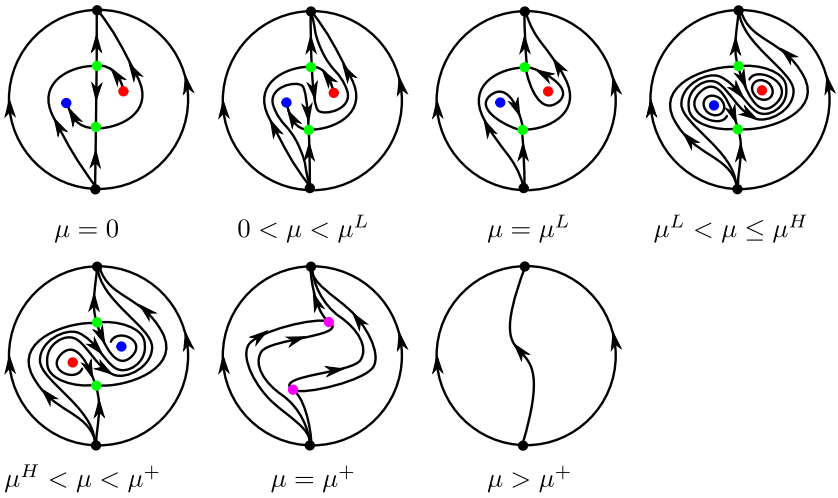

Fig. 8. Phase portraits evolution, for $\mu \geq 0$ when $(a, b) \in \mathcal{R}_{11}^-$.

Assume that $(a, b) \in \mathcal{R}_{11}^-$. As in the previous evolution, when $\mu = 0$, $x = 0$ is an invariant straight line (see Theorem 24), the points on this line are saddles and there are no limit cycles. Then for $\mu = \mu^L$ the system has two symmetric finite homoclinic connections. When they break, two symmetric limit cycles appear and shrink, to disappear in two simultaneous Hopf bifurcations for $\mu = \mu^H$, see Theorem 26. Then the symmetric pair of saddle and anti-saddle points collide in two symmetric saddle points when $\mu = \mu^+$. Afterwards, $\mu > \mu^+$, the system has no finite singular points.

Theorem 26 provides the existence of $\mu_H < 0$ ($\mu^H > 0$) for any (a, b) in $\mathcal{R}_{11}^+$ ($\mathcal{R}_{11}^-$). Consequently the Hopf surface projects the full region $\mathcal{R}_{11}^{\pm}$. Theorem 25 provides existence of $\mu_L < 0$ ($\mu^L > 0$) for values (a, b), close to Γ^+ (Γ^-) in $\mathcal{R}_{11}^+$ ($\mathcal{R}_{11}^-$). We have continued numerically these homoclinic connection values to obtain a homoclinic connection surface that also projects in the full region $\mathcal{R}_{11}^{\pm}$. Theorem 24 proves the nonexistence of limit cycles in $\mathcal{R}_0^+$ and all our simulations never provide them in $\mathcal{R}_0^-$. All the results and numerical simulations given in this paper lead us to think that system (29) never exhibit limit cycles in $\mathcal{R}_0 = \mathcal{R}_0^+ \cup \mathcal{R}_0^-$. They only exist, in configuration $(1 : 1)$, in $\mathcal{R}_{11} = \mathcal{R}_{11}^+ \cup \mathcal{R}_{11}^-$.

Acknowledgments

The first author acknowledges the support of FWO Vlaanderen (Grant number G093910). The third author was supported by the MINECO/FEDER MTM2008-03437, MTM2013-40998-P and UNAB10-4E-378 grants, by the AGAUR 2014SGR568 grant, and by the European Community FP7-PEOPLE-2012-IRSES-316338 and by the FP7-PEOPLE-2012-IRSES-318999 grants. We thank Jorge Galan for numerical simulations confirming the existence of a homoclinic connection.

References

[1] P. Aguirre, J.D. Flores, E. González-Olivares, Bifurcations and global dynamics in a predator–prey model with a strong Allee effect on the prey, and a ratio-dependent functional response, Nonlinear Anal. Real World Appl. 16 (2014) 235–249.

[2] A.A. Andronov, E.A. Leontovich, I.I. Gordon, A.G. Maĭer, Qualitative Theory of Second-Order Dynamic Systems, Halsted Press (A division of John Wiley & Sons), New York, Toronto, Ont., 1973, translated from Russian by D. Louvish.
[3] A.N. Berlinskiĭ, On the behavior of the integral curves of a differential equation, Izv. Vysšh. Učhebn. Zaved. Mat. 1960 (2(15)) (1960) 3–18.
[4] G. Chen, C. Li, C. Liu, J. Llibre, The cyclicity of period annuli of some classes of reversible quadratic systems, Discrete Contin. Dyn. Syst. 16 (1) (2006) 157–177.
[5] S.-N. Chow, C. Li, Y. Yi, The cyclicity of period annuli of degenerate quadratic Hamiltonian systems with elliptic segment loops, Ergodic Theory Dynam. Systems 22 (2) (2002) 349–374.
[6] B. Coll, C. Li, R. Prohens, Quadratic perturbations of a class of quadratic reversible systems with two centers, Discrete Contin. Dyn. Syst. 24 (3) (2009) 699–729.
[7] P. De Maesschalck, F. Dumortier, Time analysis and entry-exit relation near planar turning points, J. Differential Equations 215 (2) (2005) 225–267.
[8] P. De Maesschalck, F. Dumortier, Canard solutions at non-generic turning points, Trans. Amer. Math. Soc. 358 (5) (2006) 2291–2334 (electronic).
[9] P. De Maesschalck, F. Dumortier, Canard cycles in the presence of slow dynamics with singularities, Proc. Roy. Soc. Edinburgh Sect. A 138 (2) (2008) 265–299.
[10] P. De Maesschalck, F. Dumortier, Slow-fast Bogdanov–Takens bifurcations, J. Differential Equations 250 (2) (2011) 1000–1025.
[11] F. Dumortier, Slow divergence integral and balanced canard solutions, Qual. Theory Dyn. Syst. 10 (1) (2011) 65–85.
[12] F. Dumortier, J. Llibre, J.C. Artés, Qualitative Theory of Planar Differential Systems, Universitext, Springer-Verlag, Berlin, 2006.
[13] F. Dumortier, R. Roussarie, Birth of canard cycles, Discrete Contin. Dyn. Syst. Ser. S 2 (4) (2009) 723–781.
[14] F. Dumortier, R. Roussarie, C. Rousseau, Hilbert's 16th problem for quadratic vector fields, J. Differential Equations 110 (1) (1994) 86–133.
[15] F. Dumortier, R. Roussarie, J. Sotomayor, Generic 3-parameter families of vector fields on the plane, unfolding a singularity with nilpotent linear part. The cusp case of codimension 3, Ergodic Theory Dynam. Systems 7 (3) (1987) 375–413.
[16] F. Dumortier, R. Roussarie, J. Sotomayor, H. Żołądek, Bifurcations of Planar Vector Fields: Nilpotent Singularities and Abelian Integrals, Lecture Notes in Math., vol. 1480, Springer-Verlag, Berlin, 1991.
[17] S. Gautier, L. Gavrilov, I.D. Iliev, Perturbations of quadratic centers of genus one, Discrete Contin. Dyn. Syst. 25 (2) (2009) 511–535.
[18] L. Gavrilov, The infinitesimal 16th Hilbert problem in the quadratic case, Invent. Math. 143 (3) (2001) 449–497.
[19] R. Huzak, P. De Maesschalck, F. Dumortier, Limit cycles in slow–fast codimension 3 saddle and elliptic bifurcations, J. Differential Equations 255 (11) (2013) 4012–4051.
[20] I.D. Iliev, Perturbations of quadratic centers, Bull. Sci. Math. 122 (2) (1998) 107–161.
[21] I.D. Iliev, C. Li, J. Yu, Bifurcations of limit cycles from quadratic non-Hamiltonian systems with two centres and two unbounded heteroclinic loops, Nonlinearity 18 (1) (2005) 305–330.
[22] C. Li, Z. Zhang, Remarks on 16th weak Hilbert problem for $n = 2$, Nonlinearity 15 (6) (2002) 1975–1992.
[23] F. Loray, A preparation theorem for codimension-one foliations, Ann. of Math. (2) 163 (2) (2006) 709–722.
[24] I. Nikolaev, E. Zhuzhoma, Flows on 2-Dimensional Manifolds: An Overview, Lecture Notes in Math., vol. 1705, Springer-Verlag, Berlin, 1999.
[25] L. Perko, Differential Equations and Dynamical Systems, third edition, Texts Appl. Math., vol. 7, Springer-Verlag, New York, 2001.
[26] S. Ruan Shigui, Y. Tang, W. Zhang, Versal unfoldings of predator–prey systems with ratio-dependent functional response, J. Differential Equations 249 (6) (2010) 1410–1435.
[27] L. Stolovitch, Progress in normal form theory, Nonlinearity 22 (7) (2009) R77–R99.
[28] H. Żołądek, Quadratic systems with center and their perturbations, J. Differential Equations 109 (2) (1994) 223–273.